LA-UR-20-26000
Approved for public release; distribution is unlimited.

Title: (U) Preliminary Notes on Bondarenko Self-Shielded Cross Section Sensitivities

Author(s): Favorite, Jeffrey A.

Intended for: Report

Issued: 2020-09-18 (rev.1)

Los Alamos
NATIONAL LABORATORY
memorandum
X-Computational Physics Division
Radiation Transport Applications Group
Group XCP-7, MS F663
Los Alamos, New Mexico 87545
505/667-1920

To/MS: Distribution
From/MS: Jeffrey A. Favorite / XCP-7, MS F663
Phone/Email: 7-7941 / fave@lanl.gov
Symbol: XCP-7:20–019(U) (LA–UR–20–26000)
Date: September 14, 2020 (Rev. 1)
August 5, 2020 (Rev. 0)

SUBJECT: (U) Preliminary Notes on Bondarenko Self-Shielded Cross Section Sensitivities

I. Introduction

The Bondarenko method for resonance self-shielding[1] was recently implemented[2] in the PARTISN multigroup discrete ordinates code.[3] This report derives the sensitivities of self-shielded cross sections with respect to nuclide densities and the subsequent sensitivities of k_{eff} with respect to nuclide densities. Numerical results are presented for two test problems.

Williams et al.[4] developed the formalism for *explicit* and *implicit* effects on a response, meaning those effects that appear explicitly or implicitly in the transport equation. For example, a response depends explicitly on nuclide densities through the macroscopic transport cross sections but also implicitly on nuclide densities because the resonance self-shielded microscopic cross sections depend on them.

In Ref. 4, the implicit sensitivity requires accounting for Bondarenko weight functions in a cross section processing code. In the PARTISN implementation,[2] cross section processing is done in advance and is not available when the material compositions become known to the transport code. In the derivation that follows, the implicit sensitivity is analytic and uses the tabulated background cross sections.

The sensitivities of self-shielded cross sections with respect to nuclide densities have been implemented in a stand-alone computer code. A development version of the SENSMG code[5,6] computes explicit and implicit sensitivities separately, and the total sensitivity is computed in post-processing. This work will eventually lead to the calculation of total sensitivities in SENSMG.

The next section of this report describes the implementation of the Bondarenko method in PARTISN. Section III derives the derivative of the self-shielded microscopic nuclide cross sections with respect to nuclide densities, and Section IV derives the derivative of the self-shielded macroscopic material cross sections with respect to nuclide densities. Section V applies these derivatives to the k_{eff} sensitivities. Section VI discusses the preliminary implementation of these equations in a stand-alone code and in SENSMG. Section VII presents verification results from two test problems. Section VIII is a summary and discusses future work. Appendix A proves some interesting facts about the sums of the derivatives. The input files used for verification are listed in Appendix B.

II. The Bondarenko Method in PARTISN

The first step in the Bondarenko method is to read the background cross sections $\hat{\sigma}_{t,i}^{g}(\hat{s}_{0,h})$ for $g = 1,\ldots,G$ energy groups, $i = 1,\ldots,I$ nuclides in the material, and $h = 1,\ldots,H$ background cross section points $\hat{s}_{0,h}$. (In Ref. 2, $\hat{s}_{0,h}$ has *i* and *g* indices for generality, but in practice the $\hat{s}_{0,h}$ values do not depend on *i* and *g*). The hat indicates table values.

The iteration (which is a fixed-point iteration[7]) begins by setting the background cross sections and total microscopic cross sections to their infinite-dilution values, $\sigma_{b,i}^{g} = \hat{s}_{0,H}$ and $\sigma_{t,i}^{g} = \hat{\sigma}_{t,i}^{g}(\hat{s}_{0,H})$, and computing the material macroscopic cross section $\Sigma_{t,m}^{g}$ in energy group *g* for material *m* using the standard equation,

$$\Sigma_{t,m}^{g} = \sum_{i=1}^{I} N_i \hat{\sigma}_{t,i}^{g}(\hat{s}_{0,H}), \tag{1}$$

where N_i is the density of nuclide *i*. Then compute the new background cross sections using

$$\sigma_{b,i}^{g} = \frac{1}{N_i}\left(\Sigma_{t,m}^{g} - N_i \hat{\sigma}_{t,i}^{g}(\hat{s}_{0,H}) + \Sigma_{e,m}^{g}\right), \tag{2}$$

where $\Sigma_{e,m}^{g}$ is a user-input "escape cross section" for material *m* that is introduced to approximately account for spatial effects. In Ref. 2 and in this report, it is assumed that $\Sigma_{e,m}^{g}$ does not depend on nuclide properties, but it can be different in different geometric regions or materials (hence the subscript *m*). (In Ref. 2, the escape cross section does not depend on the energy group *g*.)

Compute the new microscopic total cross sections using a square-root interpolation on the background cross-section grid, using the endpoints of the grid if necessary, rather than extrapolating off the grid:

$$\sigma_{t,i}^{g}(\sigma_{b,i}^{g}) = \begin{cases} \hat{\sigma}_{t,i}^{g}(\hat{s}_{0,1}), & \sigma_{b,i}^{g} \le \hat{s}_{0,1} \\ \hat{\sigma}_{t,i}^{g}(\hat{s}_{0,h-1}) + \dfrac{\hat{\sigma}_{t,i}^{g}(\hat{s}_{0,h}) - \hat{\sigma}_{t,i}^{g}(\hat{s}_{0,h-1})}{\sqrt{\hat{s}_{0,h}} - \sqrt{\hat{s}_{0,h-1}}}\left(\sqrt{\sigma_{b,i}^{g}} - \sqrt{\hat{s}_{0,h-1}}\right), & \hat{s}_{0,h-1} < \sigma_{b,i}^{g} \le \hat{s}_{0,h} \\ \hat{\sigma}_{t,i}^{g}(\hat{s}_{0,H}), & \hat{s}_{0,H} < \sigma_{b,i}^{g}. \end{cases} \tag{3}$$

Compute the new material macroscopic cross section using

$$\Sigma_{t,m}^{g} = \sum_{i=1}^{I} N_i \sigma_{t,i}^{g}(\sigma_{b,i}^{g}) \tag{4}$$

and new background cross sections using

$$\begin{aligned} \sigma_{b,i}^{g} &= \frac{1}{N_i}\left(\Sigma_{t,m}^{g} - N_i \sigma_{t,i}^{g}(\sigma_{b,i}^{g}) + \Sigma_{e,m}^{g}\right) \\ &= \frac{\Sigma_{t,m}^{g}}{N_i} - \sigma_{t,i}^{g}(\sigma_{b,i}^{g}) + \frac{\Sigma_{e,m}^{g}}{N_i} \\ &= (\sigma_{b,i}^{g})_k \end{aligned} \tag{5}$$

for iteration k. If $\left|\frac{(\sigma_{b,i}^g)_k}{(\sigma_{b,i}^g)_{k-1}}-1\right|$ > BEPSI (a user-input convergence criterion[3]) for any nuclide i or energy group g, repeat Eqs. (3), (4), and (5). For $\sigma_{b,i}^g$ outside the bounds of the grid (i.e., $\sigma_{b,i}^g \le \hat{s}_{0,1}$ or $\hat{s}_{0,H} < \sigma_{b,i}^g$), $\sigma_{b,i}^g$ convergence is not checked.

Once the background cross sections are converged, all transport cross sections and the fission χ matrix are resonance self-shielded using Eq. (3):

$$\sigma_{x,i}^g(\sigma_{b,i}^g) = \begin{cases} \hat{\sigma}_{x,i}^g(\hat{s}_{0,1}), & \sigma_{b,i}^g \le \hat{s}_{0,1} \\ \hat{\sigma}_{x,i}^g(\hat{s}_{0,h-1}) + \left[\hat{\sigma}_{x,i}^g(\hat{s}_{0,h}) - \hat{\sigma}_{x,i}^g(\hat{s}_{0,h-1})\right] b_i^g\,, & \hat{s}_{0,h-1} < \sigma_{b,i}^g \le \hat{s}_{0,h} \\ \hat{\sigma}_{x,i}^g(\hat{s}_{0,H}), & \hat{s}_{0,H} < \sigma_{b,i}^g, \end{cases} \tag{6}$$

where the interpolation factor b_i^g,

$$b_i^g \equiv \frac{\sqrt{\sigma_{b,i}^g} - \sqrt{\hat{s}_{0,h-1}}}{\sqrt{\hat{s}_{0,h}} - \sqrt{\hat{s}_{0,h-1}}}, \; \hat{s}_{0,h-1} < \sigma_{b,i}^g \le \hat{s}_{0,h}, \tag{7}$$

is constant for all reactions for nuclide i and energy group g.

For the calculations discussed in Ref. 2, total microscopic cross sections for $H = 6$ background cross sections were tabulated: $\hat{s}_{0,h}$ = {10^{-1}, 10^1, 10^2, 10^3, 10^4, 10^{10}} (units are barns). These tables are based on ENDF/B-VII, they are available in 618 groups, and they can be collapsed. The GENDIR file for this library is /usr/projects/lindet/xsec/selfshielding/gendir. A 44-group library based on ENDF/B-VIII.0 is also available.[8] It has $H = 10$ background cross sections tabulated: $\hat{s}_{0,h}$ = {10^1, 3×10^1, 10^2, 3×10^2, 10^3, 3×10^3, 10^4, 3×10^4, 10^5, 10^{10}} (units are barns). The GENDIR file for this library is /usr/projects/data/nuclear/ndi/special/e8g44s/gendir_all.

In the libraries, the $\hat{\sigma}_{t,i}^g(\hat{s}_{0,H})$ are the infinite-dilution cross sections.

III. Derivative of the Self-Shielded Microscopic Nuclide Cross Sections with Respect to Nuclide Density

When the background cross sections are converged, Eq. (3) is satisfied. From Eq. (3), the derivative of the microscopic total cross section for nuclide i with respect to the density of nuclide j is

$$\frac{\partial \sigma_{t,i}^g}{\partial N_j} = \begin{cases} 0, & \sigma_{b,i}^g \le \hat{s}_{0,1} \\ \dfrac{1}{2\sqrt{\sigma_{b,i}^g}} \dfrac{\hat{\sigma}_{t,i}^g(\hat{s}_{0,h}) - \hat{\sigma}_{t,i}^g(\hat{s}_{0,h-1})}{\sqrt{\hat{s}_{0,h}} - \sqrt{\hat{s}_{0,h-1}}} \dfrac{\partial \sigma_{b,i}^g}{\partial N_j}, & \hat{s}_{0,h-1} < \sigma_{b,i}^g \le \hat{s}_{0,h} \\ 0, & \hat{s}_{0,H} < \sigma_{b,i}^g, \end{cases} \tag{8}$$
$$i = 1,\dots I,\; j = 1,\dots I,\; g = 1,\dots G.$$

It will be convenient to define

$$f_i^g \equiv \frac{1}{2\sqrt{\sigma_{b,i}^g}} \frac{\hat{\sigma}_{t,i}^g(\hat{s}_{0,h}) - \hat{\sigma}_{t,i}^g(\hat{s}_{0,h-1})}{\sqrt{\hat{s}_{0,h}} - \sqrt{\hat{s}_{0,h-1}}}. \tag{9}$$

From the second line of Eq. (5), the derivative of the microscopic background cross section for nuclide i with respect to the density of nuclide j is

$$\frac{\partial \sigma_{b,i}^g}{\partial N_j} = -\frac{\delta_{ij}}{N_i^2}(\Sigma_{t,m}^g + \Sigma_{e,m}^g) + \frac{1}{N_i}\sigma_{t,j}^g(\sigma_{b,j}^g) + \frac{1}{N_i}\sum_{k=1}^{I} N_k \frac{\partial \sigma_{t,k}^g}{\partial N_j} - \frac{\partial \sigma_{t,i}^g}{\partial N_j}, \tag{10}$$

where δ_{ij} is the Kronecker delta. Using Eqs. (9) and (10) in Eq. (8) yields

$$\frac{\partial \sigma_{t,i}^g}{\partial N_j} = f_i^g \left[-\frac{\delta_{ij}}{N_i^2}(\Sigma_{t,m}^g + \Sigma_{e,m}^g) + \frac{1}{N_i}\sigma_{t,j}^g(\sigma_{b,j}^g) + \frac{1}{N_i}\sum_{k=1}^{I} N_k \frac{\partial \sigma_{t,k}^g}{\partial N_j} - \frac{\partial \sigma_{t,i}^g}{\partial N_j} \right]. \tag{11}$$

Multiplying Eq. (11) by N_i, dividing by f_i^g, and rearranging yields

$$N_i \left(\frac{1+f_i^g}{f_i^g} \right) \frac{\partial \sigma_{t,i}^g}{\partial N_j} - \sum_{k=1}^{I} N_k \frac{\partial \sigma_{t,k}^g}{\partial N_j} = -\frac{\delta_{ij}}{N_i}(\Sigma_{t,m}^g + \Sigma_{e,m}^g) + \sigma_{t,j}^g(\sigma_{b,j}^g). \tag{12}$$

Applying the second line of Eq. (5) to the two terms on the right side of Eq. (12) yields

$$N_i \left(\frac{1+f_i^g}{f_i^g} \right) \frac{\partial \sigma_{t,i}^g}{\partial N_j} - \sum_{k=1}^{I} N_k \frac{\partial \sigma_{t,k}^g}{\partial N_j} = -\delta_{ij}\sigma_{b,j}^g + (1-\delta_{ij})\sigma_{t,j}^g. \tag{13}$$

Noting that

$$N_i \left(\frac{1+f_i^g}{f_i^g} \right) - N_i = \frac{N_i}{f_i^g}, \tag{14}$$

the I equations for each j and g are

$$\begin{cases} \frac{N_1}{f_1^g}\frac{\partial \sigma_{t,1}^g}{\partial N_j} - \left(N_2 \frac{\partial \sigma_{t,2}^g}{\partial N_j} + \cdots + N_I \frac{\partial \sigma_{t,I}^g}{\partial N_j} \right) = -\delta_{1j}\sigma_{b,j}^g + (1-\delta_{1j})\sigma_{t,j}^g \\ \frac{N_2}{f_2^g}\frac{\partial \sigma_{t,2}^g}{\partial N_j} - \left(N_1 \frac{\partial \sigma_{t,1}^g}{\partial N_j} + N_3 \frac{\partial \sigma_{t,3}^g}{\partial N_j} \cdots + N_I \frac{\partial \sigma_{t,I}^g}{\partial N_j} \right) = -\delta_{2j}\sigma_{b,j}^g + (1-\delta_{2j})\sigma_{t,j}^g \\ \vdots \\ \frac{N_I}{f_I^g}\frac{\partial \sigma_{t,I}^g}{\partial N_j} - \left(N_1 \frac{\partial \sigma_{t,1}^g}{\partial N_j} + N_2 \frac{\partial \sigma_{t,2}^g}{\partial N_j} + \cdots + N_{I-1} \frac{\partial \sigma_{t,I-1}^g}{\partial N_j} \right) = -\delta_{Ij}\sigma_{b,j}^g + (1-\delta_{Ij})\sigma_{t,j}^g. \end{cases} \tag{15}$$

Equation (15) can be written

$$\begin{bmatrix} N_1/f_1^g & -N_2 & \cdots & -N_I \\ -N_1 & N_2/f_2^g & \cdots & -N_I \\ \vdots & \vdots & \ddots & \vdots \\ -N_1 & -N_2 & \cdots & N_I/f_I^g \end{bmatrix} \begin{bmatrix} \partial \sigma_{t,1}^g/\partial N_j \\ \partial \sigma_{t,2}^g/\partial N_j \\ \vdots \\ \partial \sigma_{t,I}^g/\partial N_j \end{bmatrix} = \begin{bmatrix} -\delta_{1j}\sigma_{b,j}^g + (1-\delta_{1j})\sigma_{t,j}^g \\ -\delta_{2j}\sigma_{b,j}^g + (1-\delta_{2j})\sigma_{t,j}^g \\ \vdots \\ -\delta_{Ij}\sigma_{b,j}^g + (1-\delta_{Ij})\sigma_{t,j}^g \end{bmatrix}, \tag{16}$$
$$j = 1, \ldots I, g = 1, \ldots G.$$

Equation (16) represents $I \times G$ matrix equations $\underline{\underline{A}}\underline{x} = \underline{b}$, but the $\underline{\underline{A}}$ matrix only needs to be inverted G times.

It has been assumed that $\hat{\sigma}^g_{t,i}(\hat{s}_{0,h}) \neq \hat{\sigma}^g_{t,i}(\hat{s}_{0,h-1})$ in Eq. (9) and therefore $f^g_i \neq 0$, but there is no guarantee of this condition. If $f^g_i = 0$, or if the endpoints of the background cross section grid are used, then $\partial\sigma^g_{t,i} / \partial N_j = 0$ [from Eq. (8)]. The elements $A_{i,j}$ of the $\underline{\underline{A}}$ matrix of Eq. (16) and b_i of the $\underline{b}$ vector of Eq. (16) then become

$$\text{if} f^g_i = 0, \text{ then } A_{i,j} = \delta_{ij} \tag{17}$$

and

$$\text{if} f^g_i = 0, \text{ then } b_i = 0. \tag{18}$$

The derivative of the microscopic transport cross section for reaction *x* (including the elements of the fission χ matrix) for $\hat{s}_{0,h-1} < \sigma^g_{b,i} \leq \hat{s}_{0,h}$ is, from Eqs. (6) and (7),

$$\begin{aligned}\frac{\partial\sigma^g_{x,i}(\sigma^g_{b,i})}{\partial N_j} &= \left[\hat{\sigma}^g_{x,i}(\hat{s}_{0,h}) - \hat{\sigma}^g_{x,i}(\hat{s}_{0,h-1})\right]\frac{\partial b^g_i}{\partial N_j} \\ &= \frac{1}{2\sqrt{\sigma^g_{b,i}}}\frac{\hat{\sigma}^g_{x,i}(\hat{s}_{0,h}) - \hat{\sigma}^g_{x,i}(\hat{s}_{0,h-1})}{\sqrt{\hat{s}_{0,h}} - \sqrt{\hat{s}_{0,h-1}}}\frac{\partial\sigma^g_{b,i}}{\partial N_j}.\end{aligned} \tag{19}$$

The derivative for the full range of $\sigma^g_{b,i}$ is analogous to Eq. (8):

$$\frac{\partial\sigma^g_{x,i}(\sigma^g_{b,i})}{\partial N_j} = \begin{cases} 0, & \sigma^g_{b,i} \leq \hat{s}_{0,1} \\ \dfrac{1}{2\sqrt{\sigma^g_{b,i}}}\dfrac{\hat{\sigma}^g_{x,i}(\hat{s}_{0,h}) - \hat{\sigma}^g_{x,i}(\hat{s}_{0,h-1})}{\sqrt{\hat{s}_{0,h}} - \sqrt{\hat{s}_{0,h-1}}}\dfrac{\partial\sigma^g_{b,i}}{\partial N_j}, & \hat{s}_{0,h-1} < \sigma^g_{b,i} \leq \hat{s}_{0,h} \\ 0, & \hat{s}_{0,H} < \sigma^g_{b,i}, \end{cases} \tag{20}$$

$$i = 1,\ldots I, j = 1,\ldots I, g = 1,\ldots G.$$

The derivative $\partial\sigma^g_{b,i} / \partial N_j$ is obtained from Eq. (10) [after solving Eq. (16)].

It is proven in Appendix A that

$$\text{if } \Sigma^g_{e,m} = 0, \text{ then } \sum_{j=1}^{I} N_j \sum_{i=1}^{I} N_i \frac{\partial\sigma^g_{t,i}}{\partial N_j} = 0, \tag{21}$$

$$\text{if } \Sigma^g_{e,m} = 0, \text{ then } \sum_{j=1}^{I} N_j \sum_{i=1}^{I} N_i \frac{\partial\sigma^g_{b,i}}{\partial N_j} = 0, \tag{22}$$

and

$$\text{if } \Sigma^g_{e,m} = 0, \text{ then } \sum_{j=1}^{I} N_j \sum_{i=1}^{I} N_i \frac{\partial\sigma^g_{x,i}}{\partial N_j} = 0. \tag{23}$$

IV. Derivative of the Self-Shielded Macroscopic Material Cross Sections with Respect to Nuclide Density

Once the microscopic transport cross sections are resonance self-shielded, the macroscopic material transport cross sections $\Sigma^g_{x,m}$ (but not the fission χ matrix) are obtained from

$$\Sigma_{x,m}^g = \sum_{i=1}^I N_i \sigma_{x,i}^g(\sigma_{b,i}^g). \tag{24}$$

The derivative of $\Sigma_{x,m}^g$ with respect to the density N_j of nuclide *j* is

$$\frac{\partial \Sigma_{x,m}^g}{\partial N_j} = \sigma_{x,j}^g + \sum_{i=1}^I N_i \frac{\partial \sigma_{x,i}^g}{\partial N_j}. \tag{25}$$

The derivative $\partial \sigma_{x,i}^g / \partial N_j$ of the microscopic cross section is given by Eq. (19).

The first term on the right side of Eq. (25) is the derivative of $\Sigma_{x,m}^g$ in the absence of resonance self-shielding, in which case the derivatives $\partial \sigma_{x,i}^g / \partial N_j$ are zero. The second term, then, is the implicit effect of resonance self-shielding.

The macroscopic material fission χ matrix elements are obtained from

$$\chi_m^{g'\to g} = \frac{\sum_{i=1}^I \chi_i^{g'\to g} N_i \nu\sigma_{f,i}^{g'}}{\sum_{i=1}^I N_i \nu\sigma_{f,i}^{g'}} = \frac{\sum_{i=1}^I \chi_i^{g'\to g} N_i \nu\sigma_{f,i}^{g'}}{\nu\Sigma_{f,m}^{g'}}. \tag{26}$$

The derivative of $\chi_m^{g'\to g}$ with respect to the density N_j of nuclide *j* [using Eq. (25) where appropriate] is

$$\begin{aligned}\frac{\partial \chi_m^{g'\to g}}{\partial N_j} &= -\frac{\sum_{i=1}^I \chi_i^{g'\to g} N_i \nu\sigma_{f,i}^{g'}}{(\nu\Sigma_{f,m}^{g'})^2}\left(\nu\sigma_{f,j}^{g'} + \sum_{i=1}^I N_i \frac{\partial \nu\sigma_{f,i}^{g'}}{\partial N_j}\right) \\ &+ \frac{1}{\nu\Sigma_{f,m}^{g'}} \sum_{i=1}^I \left(\frac{\partial \chi_i^{g'\to g}}{\partial N_j} N_i \nu\sigma_{f,i}^{g'} + \delta_{ij}\chi_i^{g'\to g}\nu\sigma_{f,i}^{g'} + \chi_i^{g'\to g} N_i \frac{\partial \nu\sigma_{f,i}^{g'}}{\partial N_j}\right).\end{aligned} \tag{27}$$

Using Eq. (26) for the first factor on the right side term and rearranging yields

$$\begin{aligned}\frac{\partial \chi_m^{g'\to g}}{\partial N_j} &= -\frac{\chi_m^{g'\to g}}{\nu\Sigma_{f,m}^{g'}}\nu\sigma_{f,j}^{g'} + \frac{1}{\nu\Sigma_{f,m}^{g'}}\chi_j^{g'\to g}\nu\sigma_{f,j}^{g'} \\ &+ \frac{1}{\nu\Sigma_{f,m}^{g'}} \sum_{i=1}^I \left(\frac{\partial \chi_i^{g'\to g}}{\partial N_j} N_i \nu\sigma_{f,i}^{g'} + \chi_i^{g'\to g} N_i \frac{\partial \nu\sigma_{f,i}^{g'}}{\partial N_j} - \chi_m^{g'\to g} N_i \frac{\partial \nu\sigma_{f,i}^{g'}}{\partial N_j}\right) \\ &= \left(\chi_j^{g'\to g} - \chi_m^{g'\to g}\right)\frac{\nu\sigma_{f,j}^{g'}}{\nu\Sigma_{f,m}^{g'}} \\ &+ \frac{1}{\nu\Sigma_{f,m}^{g'}} \sum_{i=1}^I N_i \left(\frac{\partial \chi_i^{g'\to g}}{\partial N_j}\nu\sigma_{f,i}^{g'} + \left[\chi_i^{g'\to g} - \chi_m^{g'\to g}\right]\frac{\partial \nu\sigma_{f,i}^{g'}}{\partial N_j}\right).\end{aligned} \tag{28}$$

The derivatives $\partial \nu\sigma_{f,i}^g / \partial N_j$ and $\partial \chi_i^{g'\to g} / \partial N_j$ are given by Eq. (19).

The first term on the right side of Eq. (28) is the derivative of $\chi_m^{g'\to g}$ in the absence of resonance self-shielding, in which case the derivatives $\partial \nu\sigma_{f,i}^g / \partial N_j$ and $\partial \chi_i^{g'\to g} / \partial N_j$ are zero. The second term, then, is the implicit effect of resonance self-shielding.

V. Application to k_{eff} Sensitivity

The relative sensitivity S_{k,N_j} of k_{eff} to the density N_j of nuclide j is defined to be

$$S_{k,N_j} \equiv \frac{N_{j,0}}{k_{eff,0}} \frac{\partial k_{eff}}{\partial N_j}\bigg|_{N_j = N_{j,0}} . \tag{29}$$

The adjoint-based formula for S_{k,N_j} is

$$S_{k,N_j} = \frac{\int_{V_j} dV \sum_{g=1}^{G} \int_{4\pi} d\hat{\mathbf{\Omega}}\, \psi^{*g}(r,\hat{\mathbf{\Omega}})\, N_j \left(\lambda \frac{\partial F}{\partial N_j} - \frac{\partial A}{\partial N_j} \right) \psi^{g}(r,\hat{\mathbf{\Omega}})}{\int_{V} dV \sum_{g=1}^{G} \int_{4\pi} d\hat{\mathbf{\Omega}}\, \psi^{*g}(r,\hat{\mathbf{\Omega}})\, \lambda F\, \psi^{g}(r,\hat{\mathbf{\Omega}})}, \tag{30}$$

where V_j is the volume in which nuclide j appears and $\lambda = 1/k_{eff}$. In addition, A and F are the loss and fission production operators, defined as

$$A\psi = \hat{\mathbf{\Omega}} \cdot \nabla\, \psi^{g}(r,\hat{\mathbf{\Omega}}) + \Sigma_t^{g}(r)\psi^{g}(r,\hat{\mathbf{\Omega}}) - \sum_{g'=1}^{G} \int_{4\pi} d\hat{\mathbf{\Omega}}'\, \Sigma_s^{g'\to g}(r,\hat{\mathbf{\Omega}}' \to \hat{\mathbf{\Omega}})\psi^{g'}(r,\hat{\mathbf{\Omega}}') \tag{31}$$

and

$$F\psi = \sum_{g'=1}^{G} \int_{4\pi} d\hat{\mathbf{\Omega}}'\, \chi^{g'\to g}(r)\nu\Sigma_f^{g'}(r)\psi^{g'}(r,\hat{\mathbf{\Omega}}'). \tag{32}$$

In the absence of resonance self-shielding—i.e., using the first terms in Eqs. (25) and (28)—the operator derivatives are

$$\frac{\partial A}{\partial N_j}\psi = \sigma_{t,j}^{g}(r)\psi^{g}(r,\hat{\mathbf{\Omega}}) - \sum_{g'=1}^{G} \int_{4\pi} d\hat{\mathbf{\Omega}}'\, \sigma_{s,j}^{g'\to g}(r,\hat{\mathbf{\Omega}}' \to \hat{\mathbf{\Omega}})\psi^{g'}(r,\hat{\mathbf{\Omega}}') \tag{33}$$

and

$$\begin{aligned} \frac{\partial F}{\partial N_j}\psi &= \sum_{g'=1}^{G} \int_{4\pi} d\hat{\mathbf{\Omega}}'\, \chi^{g'\to g}(r)\nu\sigma_{f,j}^{g'}(r)\psi^{g'}(r,\hat{\mathbf{\Omega}}') \\ &+ \sum_{g'=1}^{G} \int_{4\pi} d\hat{\mathbf{\Omega}}' \left(\chi_j^{g'\to g}(r) - \chi^{g'\to g}(r) \right) \frac{\nu\sigma_{f,j}^{g'}(r)}{\nu\Sigma_f^{g'}(r)} \nu\Sigma_f^{g'}(r)\psi^{g'}(r,\hat{\mathbf{\Omega}}') \\ &= \sum_{g'=1}^{G} \int_{4\pi} d\hat{\mathbf{\Omega}}'\, \chi_j^{g'\to g}(r)\nu\sigma_{f,j}^{g'}(r)\psi^{g'}(r,\hat{\mathbf{\Omega}}'), \end{aligned} \tag{34}$$

assuming piecewise-constant material properties. Using Eqs. (33) and (34) in Eq. (30) yields the explicit sensitivity,

$$\left(S_{k,N_j}\right)_{explicit} = \frac{\int_{V_j} dV \sum_{g=1}^{G} \int_{4\pi} d\hat{\mathbf{\Omega}}\, \psi^{*g}(r,\hat{\mathbf{\Omega}})\, \lambda \sum_{g'=1}^{G} \int_{4\pi} d\hat{\mathbf{\Omega}}'\, N_j \chi_j^{g'\to g} \nu\sigma_{f,j}^{g'} \psi^{g'}(r,\hat{\mathbf{\Omega}}')}{\int_{V} dV \sum_{g=1}^{G} \int_{4\pi} d\hat{\mathbf{\Omega}}\, \psi^{*g}(r,\hat{\mathbf{\Omega}})\, \lambda F\, \psi^{g}(r,\hat{\mathbf{\Omega}})}$$
$$-\frac{\int_{V_j} dV \sum_{g=1}^{G} \int_{4\pi} d\hat{\mathbf{\Omega}}\, \psi^{*g}(r,\hat{\mathbf{\Omega}})\, N_j \sigma_{t,j}^{g}(r) \psi^{g}(r,\hat{\mathbf{\Omega}})}{\int_{V} dV \sum_{g=1}^{G} \int_{4\pi} d\hat{\mathbf{\Omega}}\, \psi^{*g}(r,\hat{\mathbf{\Omega}})\, \lambda F\, \psi^{g}(r,\hat{\mathbf{\Omega}})} \tag{35}$$
$$+\frac{\int_{V_j} dV \sum_{g=1}^{G} \int_{4\pi} d\hat{\mathbf{\Omega}}\, \psi^{*g}(r,\hat{\mathbf{\Omega}}) \sum_{g'=1}^{G} \int_{4\pi} d\hat{\mathbf{\Omega}}'\, N_j \sigma_{s,j}^{g'\to g}(r,\hat{\mathbf{\Omega}}'\to\hat{\mathbf{\Omega}}) \psi^{g'}(r,\hat{\mathbf{\Omega}}')}{\int_{V} dV \sum_{g=1}^{G} \int_{4\pi} d\hat{\mathbf{\Omega}}\, \psi^{*g}(r,\hat{\mathbf{\Omega}})\, \lambda F\, \psi^{g}(r,\hat{\mathbf{\Omega}})}.$$

The explicit sensitivity can be written more compactly as

$$\left(S_{k,N_j}\right)_{explicit} = \sum_{g=1}^{G} \left[\left(S_{k,F_j^g}\right)_{explicit} - \left(S_{k,T_j^g}\right)_{explicit} + \left(S_{k,S_j^g}\right)_{explicit} \right]. \tag{36}$$

Identification of the group-dependent relative sensitivities for fission, total interactions, and scattering follows from comparing Eqs. (36) and (35).

Considering only the implicit effects of resonance self-shielding—i.e., using the second terms in Eqs. (25) and (28)—the operator derivatives are

$$\frac{\partial A}{\partial N_j}\psi = \left(\sum_{i=1}^{I} N_i \frac{\partial \sigma_{t,i}^{g}}{\partial N_j} \right) \psi^{g}(r,\hat{\mathbf{\Omega}}) - \sum_{g'=1}^{G} \int_{4\pi} d\hat{\mathbf{\Omega}}' \left(\sum_{i=1}^{I} N_i \frac{\partial \sigma_{s,i}^{g'\to g}(r,\hat{\mathbf{\Omega}}'\to\hat{\mathbf{\Omega}})}{\partial N_j} \right) \psi^{g'}(r,\hat{\mathbf{\Omega}}') \tag{37}$$

and

$$\frac{\partial F}{\partial N_j}\psi = \sum_{g'=1}^{G} \int_{4\pi} d\hat{\mathbf{\Omega}}'\, \chi^{g'\to g}(r) \left(\sum_{i=1}^{I} N_i \frac{\partial \nu\sigma_{f,i}^{g}}{\partial N_j} \right) \psi^{g'}(r,\hat{\mathbf{\Omega}}')$$
$$+\sum_{g'=1}^{G} \int_{4\pi} d\hat{\mathbf{\Omega}}'\, \frac{1}{\nu\Sigma_f^{g'}(r)} \sum_{i=1}^{I} N_i \left(\frac{\partial \chi_i^{g'\to g}}{\partial N_j} \nu\sigma_{f,i}^{g'} + \left[\chi_i^{g'\to g} - \chi^{g'\to g} \right] \frac{\partial \nu\sigma_{f,i}^{g'}}{\partial N_j} \right) \nu\Sigma_f^{g'}(r) \psi^{g'}(r,\hat{\mathbf{\Omega}}')$$
$$= \sum_{g'=1}^{G} \int_{4\pi} d\hat{\mathbf{\Omega}}' \sum_{i=1}^{I} N_i \left(\frac{\partial \chi_i^{g'\to g}}{\partial N_j} \nu\sigma_{f,i}^{g'} + \chi_i^{g'\to g} \frac{\partial \nu\sigma_{f,i}^{g'}}{\partial N_j} \right) \psi^{g'}(r,\hat{\mathbf{\Omega}}'). \tag{38}$$

assuming piecewise-constant material properties. Using Eqs. (37) and (38) in Eq. (30) yields the implicit sensitivity,

$$\left(S_{k,N_j}\right)_{implicit} = \frac{\int_{V_j} dV \sum_{g=1}^{G} \int_{4\pi} d\hat{\mathbf{\Omega}} \psi^{*g}(r,\hat{\mathbf{\Omega}}) \lambda \sum_{g'=1}^{G} \int_{4\pi} d\hat{\mathbf{\Omega}}' N_j \left(\sum_{i=1}^{I} N_i \frac{\partial \chi_i^{g' \to g}}{\partial N_j} \nu\sigma_{f,i}^{g'} \right) \psi^{g'}(r,\hat{\mathbf{\Omega}}')}{\int_{V} dV \sum_{g=1}^{G} \int_{4\pi} d\hat{\mathbf{\Omega}} \psi^{*g}(r,\hat{\mathbf{\Omega}}) \lambda F \psi^{g}(r,\hat{\mathbf{\Omega}})}$$
$$+ \frac{\int_{V_j} dV \sum_{g=1}^{G} \int_{4\pi} d\hat{\mathbf{\Omega}} \psi^{*g}(r,\hat{\mathbf{\Omega}}) \lambda \sum_{g'=1}^{G} \int_{4\pi} d\hat{\mathbf{\Omega}}' N_j \left(\sum_{i=1}^{I} N_i \chi_i^{g' \to g} \frac{\partial \nu\sigma_{f,i}^{g'}}{\partial N_j} \right) \psi^{g'}(r,\hat{\mathbf{\Omega}}')}{\int_{V} dV \sum_{g=1}^{G} \int_{4\pi} d\hat{\mathbf{\Omega}} \psi^{*g}(r,\hat{\mathbf{\Omega}}) \lambda F \psi^{g}(r,\hat{\mathbf{\Omega}})}$$
$$- \frac{\int_{V_j} dV \sum_{g=1}^{G} \int_{4\pi} d\hat{\mathbf{\Omega}} \psi^{*g}(r,\hat{\mathbf{\Omega}}) N_j \left(\sum_{i=1}^{I} N_i \frac{\partial \sigma_{t,i}^{g}}{\partial N_j} \right) \psi^{g}(r,\hat{\mathbf{\Omega}})}{\int_{V} dV \sum_{g=1}^{G} \int_{4\pi} d\hat{\mathbf{\Omega}} \psi^{*g}(r,\hat{\mathbf{\Omega}}) \lambda F \psi^{g}(r,\hat{\mathbf{\Omega}})} \tag{39}$$
$$+ \frac{\int_{V_j} dV \sum_{g=1}^{G} \int_{4\pi} d\hat{\mathbf{\Omega}} \psi^{*g}(r,\hat{\mathbf{\Omega}}) \left[\sum_{g'=1}^{G} \int_{4\pi} d\hat{\mathbf{\Omega}}' N_j \left(\sum_{i=1}^{I} N_i \frac{\partial \sigma_{s,i}^{g' \to g}(r,\hat{\mathbf{\Omega}}' \to \hat{\mathbf{\Omega}})}{\partial N_j} \right) \psi^{g'}(r,\hat{\mathbf{\Omega}}') \right]}{\int_{V} dV \sum_{g=1}^{G} \int_{4\pi} d\hat{\mathbf{\Omega}} \psi^{*g}(r,\hat{\mathbf{\Omega}}) \lambda F \psi^{g}(r,\hat{\mathbf{\Omega}})}.$$

The implicit sensitivity can be written more compactly as

$$\left(S_{k,N_j}\right)_{implicit} = \sum_{g=1}^{G} \left[\left(S_{k,F_j^g}\right)_{implicit} - \left(S_{k,T_j^g}\right)_{implicit} + \left(S_{k,S_j^g}\right)_{implicit} \right]. \tag{40}$$

Identification of the group-dependent relative implicit sensitivities for fission, total interactions, and scattering follows from comparing Eqs. (40) and (39). (The relative implicit sensitivity for fission is the sum of the $\partial \chi_i^{g' \to g} / \partial N_j$ terms and the $\partial \nu\sigma_{f,i}^{g'} / \partial N_j$ terms.)

The total sensitivity $\left(S_{k,N_j}\right)_{total}$ is the sum of the explicit and implicit sensitivities:

$$\left(S_{k,N_j}\right)_{total} = \left(S_{k,N_j}\right)_{explicit} + \left(S_{k,N_j}\right)_{implicit}. \tag{41}$$

In Williams et al.'s formulation,[4] the total sensitivity is also the sum of the explicit and implicit components. However, the implicit sensitivity is the product of relative sensitivities, one of which has an analytic component, as in this report. For example, the implicit effect of the change in ^{1}H concentration in a uranium system is

$$\left(S_{k,N_{^1\mathrm{H}}}\right)_{implicit} = \sum_{g=1}^{G} S_{k,\sigma_{c,^{238}\mathrm{U}}^{g}} S_{\sigma_{c,^{238}\mathrm{U}}^{g},N_{^1\mathrm{H}}}, \tag{42}$$

where $\sigma_{c,^{238}\mathrm{U}}^{g}$ is the capture cross section of ^{238}U in group *g*. [Equation (42) is the implicit part of Eq. (48) from Ref. 4.] The relative sensitivity of *keff* to $\sigma_{c,^{238}\mathrm{U}}^{g}$, $S_{k,\sigma_{c,^{238}\mathrm{U}}^{g}}$, is calculated using the usual adjoint formulation, Eq. (30), except the operator derivatives are with respect to $\sigma_{c,^{238}\mathrm{U}}^{g}$ rather than N_j. The relative sensitivity of $\sigma_{c,^{238}\mathrm{U}}^{g}$ to $N_{^1\mathrm{H}}$, $S_{\sigma_{c,^{238}\mathrm{U}}^{g},N_{^1\mathrm{H}}}$, is calculated using the analytic derivative of

Eq. (5), as in this report, multiplied by a combination of integrals of the ^{1}H, ^{238}U, and background cross sections over the energy range corresponding to group g that accounts for the Bondarenko weight function. In this report (Sec. II, summarizing Ref. 2), the Bondarenko weight function is accounted for approximately in the fixed-point iteration scheme.

Because of Eqs. (21), (22), and (23), if the escape cross section is zero, then the sum over nuclides of the implicit sensitivities to nuclide densities is zero.

VI. Preliminary Implementation

The Bondarenko method as described in Sec. II was implemented in PARTISN by T. G. Saller.[2] When PARTISN writes the macroscopic material cross sections to the macrxs file, they are resonance self-shielded. PARTISN does not write nuclide microscopic cross sections to any output file (whether self-shielded or not). SENSMG obtains nuclide microscopic cross sections from PARTISN using a special PARTISN input file that has one nuclide in each zone. That method will not work for resonance self-shielded microscopic nuclide cross sections because those cross sections depend on the material composition. Thus, SENSMG will need to replicate the Bondarenko self-shielding method that is implemented in PARTISN. This will require reading the Nuclear Data Interface (NDI) files for the background cross section grid and microscopic transport cross sections, including the fission χ matrix.

For now, the Bondarenko method has been implemented in a stand-alone test code. The background cross section grid and microscopic cross sections were written to a set of ASCI text files using SENSMG's cross-section writing capability[5] ("-wrxsecs yes"). These files also contain the material compositions.

The standalone code reads the background cross section grid, microscopic total cross sections, and material compositions and computes resonance self-shielded microscopic total cross sections, background cross sections, and macroscopic total material cross sections using Eqs, (1) through (5). Then it computes the self-shielded isotopic absorption, fission production ($\nu\sigma_f$), and scattering cross sections and the fission χ matrices using Eq. (6). It writes these cross sections in a macrxs file in which each nuclide comprises a single material. Material-dependent escape cross sections are hard-wired into the stand-alone code.

The code computes the material macroscopic self-shielded absorption, fission production ($\nu\sigma_f$), and scattering cross sections using Eq. (24) and the material fission χ matrices using Eq. (26). These are output to text files and can be compared directly to the PARTISN material cross section outputs.

The code computes the derivative of the microscopic self-shielded total cross sections using Eq. (16) and the derivative of the background cross sections using Eq. (10). The derivative of the other microscopic self-shielded transport cross sections (including the fission χ matrices) is computed using Eq. (19).

The code computes the combinations of derivatives of the self-shielded microscopic cross sections, the sums in parentheses in Eq. (39). The $\partial\chi_i^{g'\to g}/\partial N_j$ terms and the $\partial\nu\sigma_{f,i}^{g'}/\partial N_j$ terms are summed together. These combinations of derivatives are written in another macrxs file in the same format as the self-shielded microscopic cross sections.

During this preliminary implementation, SENSMG has been modified only minimally. Material-dependent escape cross sections are hard-wired into the subroutine that writes PARTISN input files. The subroutine that computes the explicit sensitivities of a response to nuclide densities was copied to a new subroutine that was modified to compute the implicit sensitivities. The original (explicit) subroutine uses the macrxs file containing nuclide cross sections; a slight modification causes it to use the self-shielded nuclide cross sections from the stand-alone code. The new (implicit) subroutine uses the macrxs file containing the sums of derivatives where the cross sections should be. The formulas are the same and the subroutine doesn't know the difference. Implicit sensitivities are written to a new output file.

In this preliminary implementation, the following method is used to obtain implicit sensitivities. A development version of SENSMG allows "-sshield 1" on the command line, invoking PARTISN's "sshield=1" in block 3. The forward and adjoint calculations are done with self-shielded macroscopic transport cross sections. However, the self-shielded nuclide cross sections are not immediately available to SENSMG, as discussed previously. To use self-shielded nuclide cross sections, replace the default SENSMG nuclide cross sections (the macrxs file in the xs1 directory) with the self-shielded nuclide cross sections computed using the stand-alone code. Also ensure that there is a link to the macrxs file of derivative information in the xs1 directory. Then run SENSMG using the previously computed fluxes using the "-use_existing yes" option on the command line.[5] This yields the explicit relative sensitivities of Eq. (36) and the implicit relative sensitivities of Eq. (40). The total sensitivity is calculated in post-processing using the sum of implicit and explicit sensitivities, Eq. (41).

This capability was tested with a development version of PARTISN, version 8.32.27.

VII. Numerical Results

VII.A. UO_2 Sphere with Water

The first test problem is the two-region one-dimensional sphere presented in Sec. 5.2 of Ref. 2. The materials are defined in Table I and dimensions are shown there and in Figure 1.

Table I. Materials and Geometry of the UO_2 Sphere with Water.

Index	Material	Density [at/(b·cm)]	Density (g/cm^3)	Outer Radius (cm)
1	UO_2	^{235}U 0.004903468; ^{238}U 0.019613872; ^{16}O 0.049034681	10.96940920	35
2	Water	^{1}H 0.066656016; ^{16}O 0.033328008	0.99674881	45

The calculations used the ENDF/B-VII cross section libraries with $H = 6$ background cross sections created for Ref. 2. Thirty energy groups were used.

The derivatives $\partial\sigma_{t,i}^{g} / \partial N_j$ computed using the equations of this report (with $\Sigma_{e,m}^{g} = 0$) were verified against central differences in Ref. 9.

This report focuses on sensitivities of k_{eff}. Transport calculations were done with PARTISN 8.32.27 with S_{64} quadrature, P_3 scattering, and a convergence criterion (PARTISN's `epsi`) of 1E-6. These parameters were set on the SENSMG input line. The fine mesh spacing was 0.005 cm for both regions. The calculations used 24 processors. The SENSMG input file is listed in Appendix B.

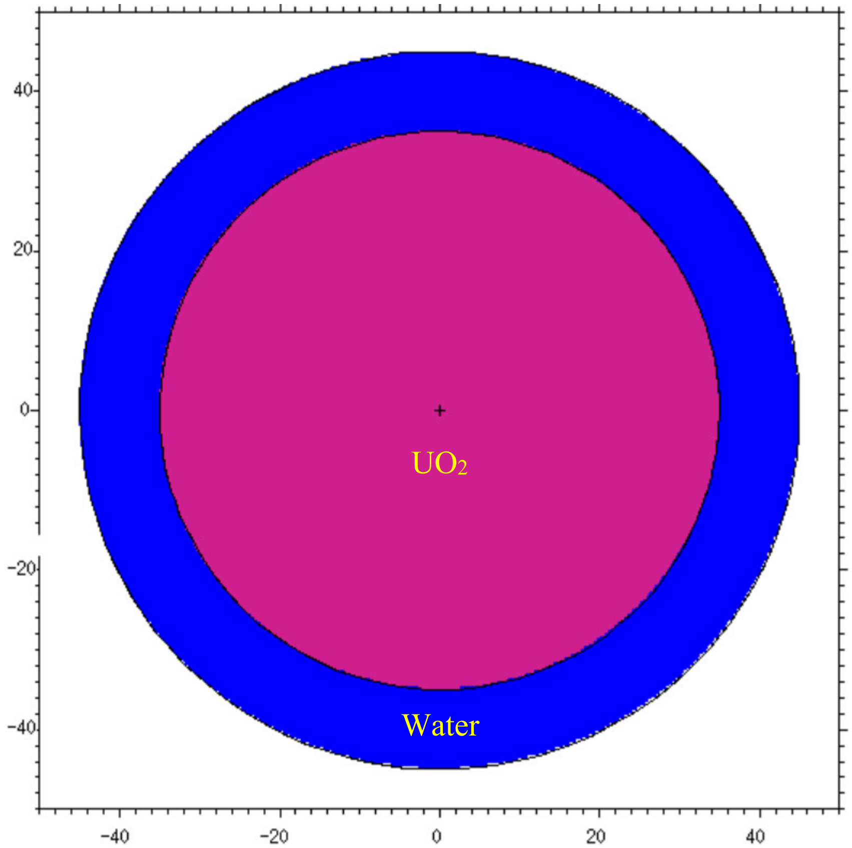

Figure 1. Cross-section of the spherical geometry. Scales in centimeters.

Total relative sensitivities computed using SENSMG [adding the explicit and implicit sensitivities as in Eq. (41)] are compared to total relative sensitivities estimated using direct perturbations in central differences in Table II. The agreement is excellent.

Table II. Total Relative Sensitivity of k_{eff} to Nuclide Density for the UO_2 Sphere with Water ($\Sigma^g_{e,m} = 0$).

Material	Nuclide	Central Difference (%/%)	Adjoint (%/%)	Difference (%)
UO_2	^{235}U	3.34480E-01	3.34479E-01	–0.0001
	^{238}U	–5.30517E-02	–5.30631E-02	0.0216
	^{16}O	3.93075E-02	3.92999E-02	–0.0194
Water	^{1}H	1.68540E-02	1.68627E-02	0.0513
	^{16}O	2.68124E-02	2.68137E-02	0.0048

The explicit and implicit relative sensitivities are compared in Table III. In the UO_2, the implicit sensitivity reduces the ^{238}U density sensitivity by 10% (in magnitude) and the ^{16}O density sensitivity by 7% (in magnitude). In the water, the implicit sensitivity reduces the ^{16}O density sensitivity by almost 2% (in magnitude) but it increases the ^{1}H density sensitivity by almost 3%.

Table III. Adjoint Explicit, Implicit, and Total Relative Sensitivity of k_{eff} to Nuclide Density for the UO_2 Sphere with Water ($\Sigma_{e,m}^{g}$ = 0).

Material	Nuclide	Explicit (%/%)	Implicit (%/%)	Total (%/%)	Fraction That Is Implicit (%)
UO_2	^{235}U	3.37045E-01	–2.56552E-03	3.34479E-01	–0.77
	^{238}U	–5.83957E-02	5.33252E-03	–5.30631E-02	–10.05
	^{16}O	4.20669E-02	–2.76700E-03	3.92999E-02	–7.04
Water	^{1}H	1.64210E-02	4.41639E-04	1.68627E-02	2.62
	^{16}O	2.72554E-02	–4.41641E-04	2.68137E-02	–1.65

Table IV compares central-difference estimates of the implicit relative sensitivities with the adjoint sensitivities from SENSMG. In the direct perturbation method, there is no way to separate the implicit and explicit sensitivities. The central-difference estimates are the central-difference estimates of the total sensitivities from Table II minus the adjoint explicit sensitivities from Table III.

For some nuclides on Table IV, the difference between the central difference and the adjoint is larger than is desirable. There is evidence that the adjoint results are correct. As mentioned in Sec. V, the sum of the implicit sensitivity to nuclide density over all the nuclides in a material is zero when $\Sigma_{e,m}^{g}$ = 0. In Table IV, the sum of the nuclide implicit sensitivity for each material is much closer to zero for the adjoint than for the central difference.

Table IV. Implicit Relative Sensitivity of k_{eff} to Nuclide Density for the UO_2 Sphere with Water ($\Sigma_{e,m}^{g}$ = 0).

Material	Nuclide	Central Difference (%/%)	Adjoint (%/%)	Difference (%)
UO_2	^{235}U	–2.56530E-03	–2.56552E-03	0.0085
	^{238}U	5.34397E-03	5.33252E-03	–0.2143
	^{16}O	–2.75936E-03	–2.76700E-03	0.2769
Water	^{1}H	4.33000E-04	4.41639E-04	1.9951
	^{16}O	–4.42930E-04	–4.41641E-04	–0.2909

In Ref. 2, Saller did this problem with escape cross sections, but noted that they had little impact on k_{eff}. The escape cross sections are $\Sigma_{e,m}^{g} = A/(4V)$, where A is the surface area bounding the region enclosing material m and V is the volume of material m. Using the radii given in Table I gives $\Sigma_{e,1}^{g}$ = 0.021428571 cm^{-1} and $\Sigma_{e,2}^{g}$ = 0.050518135 cm^{-1}. Using these escape cross sections in the present calculations reduced k_{eff} from 1.1688603 to 1.1686531, a decrease of 21 pcm.

Total relative sensitivities computed using SENSMG [adding the explicit and implicit sensitivities as in Eq. (41)] with $\Sigma_{e,m}^{g} > 0$ are compared to total relative sensitivities estimated using direct perturbations in central differences in Table V. The agreement is excellent.

The explicit and implicit relative sensitivities are compared in Table VI. Results are similar to those of Table III. Table VII compares central-difference estimates of the implicit relative sensitivities with the adjoint sensitivities from SENSMG. Results are similar to those of Table IV.

Table V. Total Relative Sensitivity of k_{eff} to Nuclide Density for the UO_2 Sphere with Water ($\Sigma_{e,m}^{g} > 0$).

Material	Nuclide	Central Difference (%/%)	Adjoint (%/%)	Difference (%)
UO_2	^{235}U	3.35014E-01	3.34995E-01	–0.0057%
	^{238}U	–5.36002E-02	–5.36055E-02	0.0099%
	^{16}O	3.94942E-02	3.94915E-02	–0.0067%
Water	^{1}H	1.67158E-02	1.67110E-02	–0.0289%
	^{16}O	2.67873E-02	2.67893E-02	0.0078%

Table VI. Adjoint Explicit, Implicit, and Total Relative Sensitivity of k_{eff} to Nuclide Density for the UO_2 Sphere with Water ($\Sigma_{e,m}^{g} > 0$).

Material	Nuclide	Explicit (%/%)	Implicit (%/%)	Total (%/%)	Fraction That Is Implicit (%)
UO_2	^{235}U	3.37427E-01	–2.43184E-03	3.34995E-01	–0.73%
	^{238}U	–5.86500E-02	5.04450E-03	–5.36055E-02	–9.41%
	^{16}O	4.19314E-02	–2.43988E-03	3.94915E-02	–6.18%
Water	^{1}H	1.62737E-02	4.37245E-04	1.67110E-02	2.62%
	^{16}O	2.72435E-02	–4.54133E-04	2.67893E-02	–1.70%

Table VII. Implicit Relative Sensitivity of k_{eff} to Nuclide Density for the UO_2 Sphere with Water ($\Sigma_{e,m}^{g} > 0$).

Material	Nuclide	Central Difference (%/%)	Adjoint (%/%)	Difference (%)
UO_2	^{235}U	–2.41290E-03	–2.43184E-03	0.7851%
	^{238}U	5.04983E-03	5.04450E-03	–0.1055%
	^{16}O	–2.43724E-03	–2.43988E-03	0.1084%
Water	^{1}H	4.42080E-04	4.37245E-04	–1.0938%
	^{16}O	–4.56230E-04	–4.54133E-04	–0.4596%

VII.B. Green Block Critical Experiment

The second test problem is the one-region one-dimensional sphere presented by Williams et al. in Sec. VII of Ref. 4. The material is defined in Table VIII. Reference 4 describes the material in terms of enrichment and hydrogen-to-^{235}U ratio but gives no densities; thus it is not fully specified. The composition given in Table VIII was kindly provided by B. J. Marshall and Will Wieselquist (Oak Ridge National Laboratory). It is mixture number 2 in Table I of Ref. 10; the density is the UF_4-CH_2 density multiplied by the ratio of the average assembly density to the UF_4-CH_2 density. (The mass density in Table VIII was computed using the nuclide atom densities.) This test problem was also used by Rearden,[11] who also neglected to fully specify it.

Table VIII. Materials and Geometry of the Spherical Green Block.

Index	Material	Density [at/(b·cm)]	Density (g/cm^3)	Outer Radius (cm)
1	2%-enriched UF_4 mixed with paraffin	^{12}C 1.857768E-02; ^{13}C 2.009312E-04; ^{19}F 2.628098E-02; ^{235}U 1.330519E-04; ^{238}U 6.437193E-03; ^{1}H 3.905952E-02	3.865389403	38.5

Using "a 199-group library processed from ENDF/B-VI using the Bondarenko method for self-shielding," and a cross section processing code for the resonance calculation, Williams et al.[4] used a discrete ordinates code to compute k_{eff} = 1.0258.

A continuous-energy and -angle MCNP6 Monte Carlo[12] calculation of the spherical Green block model was done using ENDF/B-VIII.0 cross sections and $S(\alpha,\beta)$ scattering data for polyethylene. The result was 1.00891 ± 0.00002. The input file is listed in Appendix B.

PARTISN 8.32.27 was used with S_{64} quadrature, P_3 scattering, and a convergence criterion (PARTISN's `epsi`) of 1E-6. These parameters were set on the SENSMG input line. The fine mesh spacing was 0.005 cm. The calculations used 36 processors. The SENSMG input file is listed in Appendix B. The PARTISN calculations used the 44-group ENDF/B-VIII.0 cross section libraries with H = 10 background cross sections created for Ref. 8. With no escape cross section, the result was k_{eff} = 1.04143. Using an escape cross section $\Sigma_{e,1}^{g} = A/(4V) = 0.019480519$ cm^{-1}, the result was k_{eff} = 1.03958. These cross sections do not include $S(\alpha,\beta)$ scattering, but that is not the cause of the difference between the PARTISN and MCNP results; without $S(\alpha,\beta)$ scattering, MCNP gives 1.00495 ± 0.00002.

The k_{eff} using the infinite-dilution 44-group cross sections is 0.49195. Resonance self-shielding is very important here.

The self-shielded and Monte Carlo k_{eff} results are summarized with Rearden's[11] in Table IX. The current PARTISN result is larger than the others. The weight function used to produce the 44-group library is probably not completely appropriate for this problem. (The 618-group library produced for Ref. 2 and used in Sec. VII.A cannot be used for this problem because it lacks ^{19}F.)

Table IX. k_{eff} Results for the Spherical Green Block.

Calculation	$S(\alpha,\beta)$?	Cross Section Evaluation	Number of Groups or Continuous-Energy	k_{eff}
Williams et al.[4]	Probably	ENDF/B-VI	199	1.0258
Rearden[11]	Probably	ENDF/B-V	44	1.00416 ± 0.00037
PARTISN ($\Sigma_{e,1}^{g} = 0$)	No	ENDF/B-VIII	44	1.04143
MCNP6	Yes	ENDF/B-VIII	CE	1.00891 ± 0.00002
MCNP6	No	ENDF/B-VIII	CE	1.00495 ± 0.00002

Many of the background cross sections were below the lowest grid value of 10 b. This occurred in three energy groups in ^{12}C, nine groups in ^{19}F, and 40 groups in ^{1}H. A lower grid value of 1 b would provide a more accurate interpolation for this problem.

Various calculations of the explicit and implicit relative sensitivities of k_{eff} to the density of ^{1}H are compared in Table X. The first row of Table X is directly from Table II of Williams et al.[4] The second row is directly from Table IV of Rearden.[11] The third row was computed using SENSMG, with the implicit sensitivity computed as discussed in Sec. VI. The fourth and fifth rows were computed using the iterated fission probability method in MCNP6 using the KSEN card.[12] Central differences using SENSMG and MCNP6 were computed by perturbing the ^{1}H density by ±4%, as in Ref. 4.

Table X. Explicit, Implicit, and Total Relative Sensitivity of k_{eff} to ^{1}H Density for the Spherical Green Block.

Calculation	Explicit Using Adjoint (%/%)	Implicit Using Adjoint (%/%)	Total Using Adjoint (%/%)	Total Using Central Difference (%/%)
Williams et al.[4]	0.2690	–0.0574	0.2116	0.2109
Rearden[11]	0.290 ± 2.18%	–0.066 ± 13.5%[(a)]	0.224 ± 2.78%	0.226
SENSMG ($\Sigma_{e,1}^{g} = 0$)	0.2545	–0.0556[(b)]	0.1989	0.1990
MCNP6, no $S(\alpha,\beta)$	N/A[(c)]	N/A[(c)]	0.2228 ± 0.47%	0.2214 ± 0.16%
MCNP6, with $S(\alpha,\beta)$	N/A[(c)]	N/A[(c)]	0.2194 ± 0.58%[(d)]	0.2215 ± 0.16%

(a) Computed as the difference between the total and the explicit-only results given in Table IV of Ref. 11.
(b) Using the equations of this report.
(c) There is no way to separate explicit and implicit effects using continuous-energy Monte Carlo.
(d) Includes the effect of $S(\alpha,\beta)$.

Although Table X contains results from different codes, calculation methods, and nuclear data, those results are extremely consistent. More to the point of this paper, the SENSMG results for the explicit and implicit sensitivities are 5.39% and 3.08% smaller (in magnitude), respectively than those of Williams et al. The total sensitivity is 6.02% smaller (in magnitude).

The MCNP6 results indicate that $S(\alpha,\beta)$ scattering is not an important effect in this problem.

Figure 2 compares explicit and implicit sensitivity profiles from Williams et al.[4] and SENSMG. It is difficult to compare the curves quantitatively, but qualitatively, the curves match very well.

Figure 3 compares total (i.e., the sum of explicit and implicit) sensitivities from MCNP6 and SENSMG. There is good agreement overall, but there are noticeable differences between 10^{-5} MeV and 1 MeV.

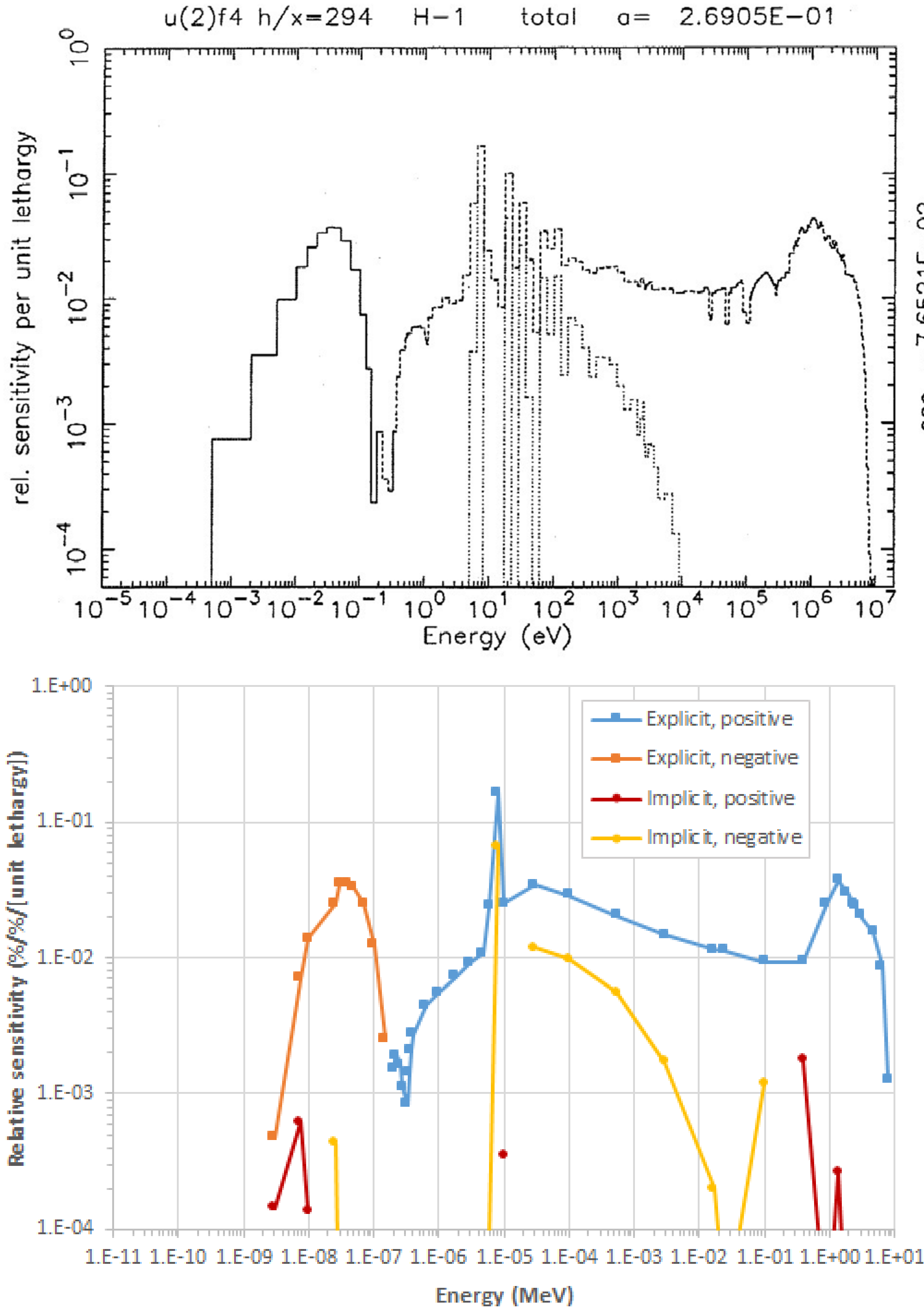

Figure 2. Relative sensitivity of k_{eff} to density of ^{1}H. (Top) Directly from Williams et al.,[4] who say “solid and dashed lines, respectively, represent negative and positive values for explicit component; dotted line represents the negative, implicit component value.” “a” is the total explicit sensitivity (c.f. Table X) and “osc” is the sum of the negative values.[11] (Bottom) From SENSMG ($\Sigma_{e,1}^{g}$ = 0).

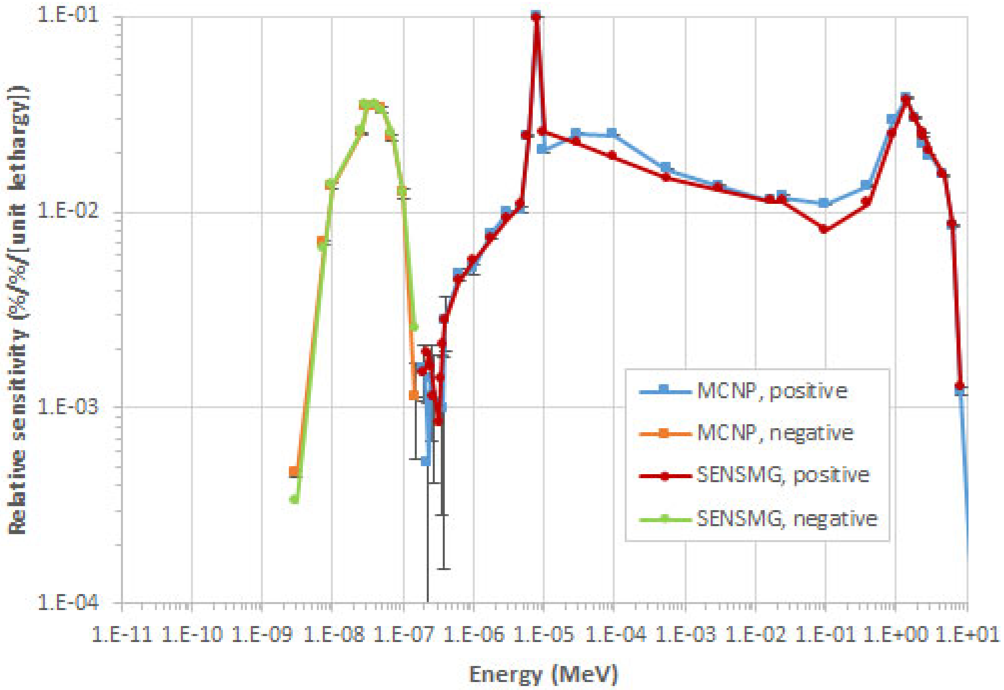

Figure 3. Total (i.e., sum of explicit and implicit effects) relative sensitivity of k_{eff} to density of ^{1}H. MCNP results have 1σ error bars. MCNP calculations do not have $S(\alpha,\beta)$. SENSMG calculations have no escape cross section.

The implicit and explicit sensitivities are compared in Table XI. The sum of the implicit sensitivities is –2.876500E-07, which is very small compared to the components; $\sum_{j=1}^{I}\left(S_{k,N_j}\right)_{implicit} \approx 0$.

Table XI. Adjoint Explicit, Implicit, and Total Relative Sensitivity of k_{eff} to Nuclide Density for the Spherical Green Block ($\Sigma_{e,1}^{g} = 0$).

Nuclide	Explicit (%/%)	Implicit (%/%)	Total (%/%)	Fraction That Is Implicit (%)
^{12}C	3.163639E-02	–7.046407E-03	2.458998E-02	–28.66%
^{13}C	3.700230E-04	–9.415265E-05	2.758704E-04	–34.13%
^{19}F	5.974718E-02	–6.898289E-03	5.284889E-02	–13.05%
^{235}U	2.558698E-01	–1.383669E-03	2.544861E-01	–0.54%
^{238}U	–2.636701E-01	7.105233E-02	–1.926178E-01	–36.89%
^{1}H	2.545006E-01	–5.563010E-02	1.988705E-01	–27.97%

This problem was also run with a non-zero escape cross section. The formula $\Sigma_{e,m}^{g} = A/(4V)$ gives $\Sigma_{e,1}^{g}$ = 0.019480519 cm^{-1}. Using this value yields k_{eff} = 1.03958, very close to the value obtained with no escape cross section, 1.04143 (Table IX). For testing purposes, a larger effect was sought. An escape cross section of $\Sigma_{e,1}^{g}$ = 0.45606939 cm^{-1} yields k_{eff} = 1.00495, the same k_{eff} obtained by MCNP6 with no $S(\alpha,\beta)$ (Table IX). The explicit, implicit, and total relative sensitivity of k_{eff} to the ^{1}H density calculated using SENSMG with $\Sigma_{e,1}^{g} = 0$ and $\Sigma_{e,1}^{g}$ = 0.45606939 cm^{-1} are compared in Table XII, and the total is compared to a central difference estimate. The central difference was computed by perturbing the ^{1}H density by ±2% rather than the ±4% used in Table X. Table IX shows that introducing a large escape cross has an effect on the sensitivities, and it verifies the equations of this report and their implementation when escape cross sections are used.

Table XII. Explicit, Implicit, and Total Relative Sensitivity of k_{eff} to ^{1}H Density Using $\Sigma_{e,1}^{g} \neq 0$ for the Spherical Green Block.

Calculation	Explicit Using Adjoint (%/%)	Implicit Using Adjoint (%/%)	Total Using Adjoint (%/%)	Total Using Central Difference (%/%)
SENSMG ($\Sigma_{e,1}^{g} = 0$)	0.2545[a]	–0.0556[a],[b]	0.1989[a]	0.1993
SENSMG ($\Sigma_{e,1}^{g} = 0.495$)	0.2787	–0.0450[a]	0.2337	0.2337

(a) Same value as in Table X.
(b) Using the equations of this report.

VIII. Summary and Future Work

A working capability to compute response sensitivities to Bondarenko self-shielded cross sections using PARTISN has been established. It is a preliminary capability not suitable for production use. It demonstrates the correctness of the equations derived in this report and the coding that implements them, and it has led to some ideas about how a production capability would be implemented in SENSMG.

It appears that a production capability will have to duplicate in SENSMG the Bondarenko method that exists in PARTISN. This is undesirable, but it is probably better than asking PARTISN to write the entire background cross section table for every nuclide.

To do this efficiently, SENSMG will have to read the NDI files. There are tools that exist for this purpose,[13] but reading the NDI directly for the weighting functions (for fission χ vectors[14]) and scattering cross sections (for diagonal and BHS transport corrections[15]) has thus far been less intimidating than learning the tools. If the self-shielding capability moves forward in SENSMG, it can only do so by using the proper tools.

It will be necessary to ensure the method of this report works with the redoin/lnk3dt capability[16] and that it works for fixed-source problems and for subcritical multiplication (Feynman Y[17]) problems. It would be useful to extend the method to second derivatives.[18]

Acknowledgments

The author would like to thank Tom Saller (LANL) for help understanding his implementation of the Bondarenko method and for providing his development version of PARTISN, B. J. Marshall (Oak Ridge National Laboratory) for providing the spherical Green block material that Williams et al. used in Ref. 4, and Keith Bledsoe (Oak Ridge National Laboratory) for discovering what "osc" means and pointing it out in Ref. 11.

References

1. I. I. Bondarenko, *Group Constants for Nuclear Reactor Calculations*, Consultants Bureau, New York (1964).

2. T. G. Saller, "Self-Shielding in PARTISN," *Proc. Int. Conf. Mathematics and Computational Methods Applied to Nuclear Science and Engineering (M&C 2019)*, 598–608, Portland, Oregon, August 25–29 (2019).

3. R. E. Alcouffe, R. S. Baker, J. A. Dahl, E. J. Davis, T. G. Saller, S. A. Turner, R. C. Ward, and R. J. Zerr, "PARTISN: A Time-Dependent, Parallel Neutral Particle Transport Code System," Los Alamos National Laboratory report LA–UR–17–29704 (Revised Sept. 2019).

4. M. L. Williams, B. L. Broadhead, and C. V. Parks, "Eigenvalue Sensitivity Theory for Resonance-Shielded Cross Sections," *Nucl. Sci. Eng.*, **138**, *2*, 177–191 (2001); https://doi.org/10.13182/NSE00-56.

5. Jeffrey A. Favorite, "SENSMG: First-Order Sensitivities of Neutron Reaction Rates, Reaction-Rate Ratios, Leakage, k_{eff}, and α Using PARTISN," *Nucl. Sci. Eng.*, **192**, *1*, 80–114 (2018); https://doi.org/10.1080/00295639.2018.1471296.

6. Jeffrey A. Favorite, "(U) SENSMG: First-Order Sensitivities of Neutron Reaction Rates, Reaction-Rate Ratios, Leakage, k_{eff}, α, and Subcritical Multiplication Using PARTISN," Rev. 1, Los Alamos National Laboratory report LA-UR-19-26249 (September 19, 2019).

7. C. T. Kelley, *Iterative Methods for Linear and Nonlinear Equations*, Chap. 1, Society for Industrial and Applied Mathematics, Philadelphia (1995); https://doi.org/10.1137/1.9781611970944.

8. Nathan A. Gibson, "Delivery of Special Purpose 44-group Nuclear Data Library," Los Alamos National Laboratory report XCP-5:20-005(U) (March 10, 2020).

9. Jeffrey A. Favorite, "Sensitivity of Bondarenko Self-Shielded Cross Sections to Nuclide Densities in PARTISN," *Transactions of the American Nuclear Society*, **123**, article in press (2020).

10. S. J. Raffety and J. T. Mihalczo, "Homogeneous Critical Assemblies of 2 and 3% Uranium-235-Enriched Uranium in Paraffin," *Nucl. Sci. Eng.*, **48**, *4*, 433–443 (1972); https://doi.org/10.13182/NSE72-A22511.

11. B. T. Rearden, "Perturbation Theory Eigenvalue Sensitivity Analysis with Monte Carlo Techniques," *Nucl. Sci. Eng.*, **146**, *3*, 367–382 (2004); https://doi.org/10.13182/NSE03-03.

12. Christopher J. Werner, ed., "MCNP® User's Manual, Code Version 6.2," Los Alamos National Laboratory report LA-UR-17-29981, Rev. 0 (Oct. 27, 2017).

13. "NDI Reference Manual, 2.0.11," generated by Doxygen 1.3.9.1 (July 20, 2009).

14. Jeffrey A. Favorite, "Differences in the Use of Isotopic χ Vectors Demonstrated with an Analytic k_∞ Problem," *Transactions of the American Nuclear Society*, **121**, 933–936 (2019).

15. Jeffrey A. Favorite, "(U) Transport Corrections Implemented in SENSMG," Los Alamos National Laboratory report LA–UR–19–28507 (August 20, 2019).

16. Jeffrey A. Favorite, "(U) LNK3DNT Capability in SENSMG Extended," Los Alamos National Laboratory report LA–UR–19–23874 (April 29, 2019).

17. Alexander R. Clark, John Mattingly, and Jeffrey A. Favorite, "Application of Neutron Multiplicity Counting Experiments to Optimal Cross Section Adjustments," *Nuclear Science and Engineering*, **194**, *4*, 308–333 (2020); https://doi.org/10.1080/00295639.2019.1698267.

18. D. G. Cacuci, R. Fang, and J. A. Favorite, "Comprehensive Second-Order Adjoint Sensitivity Analysis Methodology (2nd-ASAM) Applied to a Subcritical Experimental Reactor Physics Benchmark: I. Effects of Imprecisely Known Total and Capture Cross Sections," *Energies*, **12**, *21* (2019); https://doi.org/10.3390/en12214219.

JAF:jaf

Distribution:
J. T. Goorley, XCP-7, MS A143, jgoorley@lanl.gov
R. S. Baker, CCS-2, MS D409, rsb@lanl.gov
J. A. Dahl, CCS-2, MS D409, dahl@lanl.gov
E. J. Davis, CCS-2, MS D409, ejdavis@lanl.gov
T. Saller, CCS-2, MS D409, tgsaller@lanl.gov
R. J. Zerr, CCS-2, MS D409, rzerr@lanl.gov
R. N. Bratton, NEN-5, MS B228, bratton@lanl.gov
R. C. Little, XCP-DO, MS F663, rcl@lanl.gov
P. J. Jaegers, XTD-NTA, MS T082, pjaegers@lanl.gov
S. D. Ramsey, XTD-NTA, MS T082, ramsey@lanl.gov
T. J. Remedes, XTD-NTA, MS T082, tjremedes@lanl.gov
A. R. Clark, XCP-5, MS P365, arclark@lanl.gov
J. L. Conlin, XCP-5, MS F663, jlconlin@lanl.gov
N. A. Gibson, XCP-5, MS F644, ngibson@lanl.gov
W. Haeck, XCP-5, MS P365, wim@lanl.gov
D. Neudecker, XCP-5, MS P365, dneudecker@lanl.gov
D. K. Parsons, XCP-5, MS F663, dkp@lanl.gov
J. L. Alwin, XCP-7, MS A143, jalwin@lanl.gov
A. Sood, XCP-7, MS F663, sooda@lanl.gov
J. A. Favorite, XCP-7, MS F663, fave@lanl.gov
National Security Research Center, nsrc-cataloging@lanl.gov
XCP-7 File

Appendix A

Proof that $\sum_{j=1}^{I} N_j \sum_{i=1}^{I} N_i\, \partial\sigma_{t,i}^{g} \big/ \partial N_j = 0$ When $\Sigma_{e,m}^{g} = 0$

First we present two useful identities relating Bondarenko background and total cross sections. Using Eq. (5),

$$\begin{aligned}\sum_{i=1}^{I} N_i\sigma_{b,i}^{g} &= N_1\sigma_{b,1}^{g} + N_2\sigma_{b,2}^{g} + \cdots + N_I\sigma_{b,I}^{g} \\ &= (\Sigma_{t,m}^{g} - N_1\sigma_{t,1}^{g} + \Sigma_{e,m}^{g}) + (\Sigma_{t,m}^{g} - N_2\sigma_{t,2}^{g} + \Sigma_{e,m}^{g}) + \cdots + (\Sigma_{t,m}^{g} - N_I\sigma_{t,I}^{g} + \Sigma_{e,m}^{g}) \\ &= I\Sigma_{t,m}^{g} - \Sigma_{t,m}^{g} + I\Sigma_{e,m}^{g} \\ &= (I-1)\Sigma_{t,m}^{g} + I\Sigma_{e,m}^{g},\ g = 1,\ldots,G. \end{aligned} \tag{A.1}$$

In addition,

$$N_i\sigma_{b,i}^{g} + N_i\sigma_{t,i}^{g} = \Sigma_{t,m}^{g} + \Sigma_{e,m}^{g}, \quad i = 1,\ldots,I, g = 1,\ldots,G. \tag{A.2}$$

Because the specificity will make the derivation clearer, write Eq. (16) for $I = 4$ nuclides:

$$\begin{bmatrix} N_1/f_1^g & -N_2 & -N_3 & -N_4 \\ -N_1 & N_2/f_2^g & -N_3 & -N_4 \\ -N_1 & -N_2 & N_3/f_3^g & -N_4 \\ -N_1 & -N_2 & -N_3 & N_4/f_4^g \end{bmatrix} \begin{bmatrix} \partial\sigma_{t,1}^{g}/\partial N_j \\ \partial\sigma_{t,2}^{g}/\partial N_j \\ \partial\sigma_{t,3}^{g}/\partial N_j \\ \partial\sigma_{t,4}^{g}/\partial N_j \end{bmatrix} = \begin{bmatrix} -\delta_{1j}\sigma_{b,j}^{g} + (1-\delta_{1j})\sigma_{t,j}^{g} \\ -\delta_{2j}\sigma_{b,j}^{g} + (1-\delta_{2j})\sigma_{t,j}^{g} \\ -\delta_{3j}\sigma_{b,j}^{g} + (1-\delta_{3j})\sigma_{t,j}^{g} \\ -\delta_{4j}\sigma_{b,j}^{g} + (1-\delta_{4j})\sigma_{t,j}^{g} \end{bmatrix}, \tag{A.3}$$

$$j = 1,\ldots 4, g = 1,\ldots G.$$

For simplicity, write the $\underline{\underline{A}}$ matrix and the $\underline{b}$ vector in augmented matrix form:[19]

$$\left[\underline{\underline{A}}\ \middle|\underline{b}\right] = \left[\begin{array}{cccc|c} N_1/f_1^g & -N_2 & -N_3 & -N_4 & -\delta_{1j}\sigma_{b,j}^{g} + (1-\delta_{1j})\sigma_{t,j}^{g} \\ -N_1 & N_2/f_2^g & -N_3 & -N_4 & -\delta_{2j}\sigma_{b,j}^{g} + (1-\delta_{2j})\sigma_{t,j}^{g} \\ -N_1 & -N_2 & N_3/f_3^g & -N_4 & -\delta_{3j}\sigma_{b,j}^{g} + (1-\delta_{3j})\sigma_{t,j}^{g} \\ -N_1 & -N_2 & -N_3 & N_4/f_4^g & -\delta_{4j}\sigma_{b,j}^{g} + (1-\delta_{4j})\sigma_{t,j}^{g} \end{array}\right]. \tag{A.4}$$

Replace the fourth row of Eq. (A.4) with the difference between the third row and the fourth row:

$$\left[\underline{\underline{A}}\ \middle|\underline{b}\right] =$$

$$\left[\begin{array}{cccc|c} N_1/f_1^g & -N_2 & -N_3 & -N_4 & -\delta_{1j}\sigma_{b,j}^{g} + (1-\delta_{1j})\sigma_{t,j}^{g} \\ -N_1 & N_2/f_2^g & -N_3 & -N_4 & -\delta_{2j}\sigma_{b,j}^{g} + (1-\delta_{2j})\sigma_{t,j}^{g} \\ -N_1 & -N_2 & N_3/f_3^g & -N_4 & -\delta_{3j}\sigma_{b,j}^{g} + (1-\delta_{3j})\sigma_{t,j}^{g} \\ 0 & 0 & N_3 + N_3/f_3^g & -N_4 - N_4/f_4^g & -\delta_{3j}\sigma_{b,j}^{g} + (1-\delta_{3j})\sigma_{t,j}^{g} + \delta_{4j}\sigma_{b,j}^{g} - (1-\delta_{4j})\sigma_{t,j}^{g} \end{array}\right]. \tag{A.5}$$

Replace the third row of Eq. (A.5) with the difference between the second row and the third row:

$$\left[\underline{\underline{A}}\ \middle|\ \underline{b}\right]=\left[\begin{array}{cccc|c}
N_1/f_1^g & -N_2 & -N_3 & -N_4 & -\delta_{1j}\sigma_{b,j}^g+(1-\delta_{1j})\sigma_{t,j}^g \\
-N_1 & N_2/f_2^g & -N_3 & -N_4 & -\delta_{2j}\sigma_{b,j}^g+(1-\delta_{2j})\sigma_{t,j}^g \\
0 & N_2+N_2/f_2^g & -N_3-N_3/f_3^g & 0 & -\delta_{2j}\sigma_{b,j}^g+(1-\delta_{2j})\sigma_{t,j}^g+\delta_{3j}\sigma_{b,j}^g-(1-\delta_{3j})\sigma_{t,j}^g \\
0 & 0 & N_3+N_3/f_3^g & -N_4-N_4/f_4^g & -\delta_{3j}\sigma_{b,j}^g+(1-\delta_{3j})\sigma_{t,j}^g+\delta_{4j}\sigma_{b,j}^g-(1-\delta_{4j})\sigma_{t,j}^g
\end{array}\right]. \tag{A.6}$$

Replace the second row of Eq. (A.6) with the difference between the first row and the second row:

$$\left[\underline{\underline{A}}\ \middle|\ \underline{b}\right]=\left[\begin{array}{cccc|c}
N_1/f_1^g & -N_2 & -N_3 & -N_4 & -\delta_{1j}\sigma_{b,j}^g+(1-\delta_{1j})\sigma_{t,j}^g \\
N_1+N_1/f_1^g & -N_2-N_2/f_2^g & 0 & 0 & -\delta_{1j}\sigma_{b,j}^g+(1-\delta_{1j})\sigma_{t,j}^g+\delta_{2j}\sigma_{b,j}^g-(1-\delta_{2j})\sigma_{t,j}^g \\
0 & N_2+N_2/f_2^g & -N_3-N_3/f_3^g & 0 & -\delta_{2j}\sigma_{b,j}^g+(1-\delta_{2j})\sigma_{t,j}^g+\delta_{3j}\sigma_{b,j}^g-(1-\delta_{3j})\sigma_{t,j}^g \\
0 & 0 & N_3+N_3/f_3^g & -N_4-N_4/f_4^g & -\delta_{3j}\sigma_{b,j}^g+(1-\delta_{3j})\sigma_{t,j}^g+\delta_{4j}\sigma_{b,j}^g-(1-\delta_{4j})\sigma_{t,j}^g
\end{array}\right]. \tag{A.7}$$

Factor the atom densities on the left side of the augmented matrix and regroup cross sections on the right side:

$$\left[\underline{\underline{A}}\ \middle|\ \underline{b}\right]=\left[\begin{array}{cccc|c}
N_1/f_1^g & -N_2 & -N_3 & -N_4 & -\delta_{1j}\sigma_{b,j}^g+(1-\delta_{1j})\sigma_{t,j}^g \\
N_1(1+1/f_1^g) & -N_2(1+1/f_2^g) & 0 & 0 & (-\delta_{1j}+\delta_{2j})\sigma_{b,j}^g+[(1-\delta_{1j})-(1-\delta_{2j})]\sigma_{t,j}^g \\
0 & N_2(1+1/f_2^g) & -N_3(1+1/f_3^g) & 0 & (-\delta_{2j}+\delta_{3j})\sigma_{b,j}^g+[(1-\delta_{2j})-(1-\delta_{3j})]\sigma_{t,j}^g \\
0 & 0 & N_3(1+1/f_3^g) & -N_4(1+1/f_4^g) & (-\delta_{3j}+\delta_{4j})\sigma_{b,j}^g+[(1-\delta_{3j})-(1-\delta_{4j})]\sigma_{t,j}^g
\end{array}\right]. \tag{A.8}$$

Simplify the notation using $x_{ij}^g \equiv \partial\sigma_{t,i}^g / \partial N_j$ and write out the equations corresponding to the augmented matrix in Eq. (A.8), simplifying the right sides to yield

$$\begin{cases} N_1/f_1^g\, x_{1j}^g - N_2 x_{2j}^g - N_3 x_{3j}^g - N_4 x_{4j}^g = -\delta_{1j}\sigma_{b,j}^g + (1-\delta_{1j})\sigma_{t,j}^g \\ N_1(1+1/f_1^g)x_{1j}^g - N_2(1+1/f_2^g)x_{2j}^g = (-\delta_{1j}+\delta_{2j})(\sigma_{b,j}^g+\sigma_{t,j}^g) \\ N_2(1+1/f_2^g)x_{2j}^g - N_3(1+1/f_3^g)x_{3j}^g = (-\delta_{2j}+\delta_{3j})(\sigma_{b,j}^g+\sigma_{t,j}^g) \\ N_3(1+1/f_3^g)x_{3j}^g - N_4(1+1/f_4^g)x_{4j}^g = (-\delta_{3j}+\delta_{4j})(\sigma_{b,j}^g+\sigma_{t,j}^g). \end{cases} \tag{A.9}$$

Rearrange the fourth line of Eq. (A.9) to yield

$$N_3(1+1/f_3^g)x_{3j}^g = N_4(1+1/f_4^g)x_{4j}^g + (-\delta_{3j}+\delta_{4j})(\sigma_{b,j}^g+\sigma_{t,j}^g) \tag{A.10}$$

and

$$N_3 x_{3j}^g = \frac{N_4(1+1/f_4^g)x_{4j}^g}{(1+1/f_3^g)} + \frac{(\delta_{4j}-\delta_{3j})(\sigma_{b,j}^g+\sigma_{t,j}^g)}{(1+1/f_3^g)}. \tag{A.11}$$

Rearrange the third line of Eq. (A.9) and use Eq. (A.10) to yield

$$\begin{aligned} N_2(1+1/f_2^g)x_{2j}^g &= N_4(1+1/f_4^g)x_{4j}^g \\ &\quad + (-\delta_{3j}+\delta_{4j})(\sigma_{b,j}^g+\sigma_{t,j}^g) + (-\delta_{2j}+\delta_{3j})(\sigma_{b,j}^g+\sigma_{t,j}^g) \\ &= N_4(1+1/f_4^g)x_{4j}^g + (\delta_{4j}-\delta_{2j})(\sigma_{b,j}^g+\sigma_{t,j}^g) \end{aligned} \tag{A.12}$$

and

$$N_2 x_{2j}^g = \frac{N_4(1+1/f_4^g)x_{4j}^g}{(1+1/f_2^g)} + \frac{(\delta_{4j}-\delta_{2j})(\sigma_{b,j}^g+\sigma_{t,j}^g)}{(1+1/f_2^g)}. \tag{A.13}$$

Rearrange the second line of Eq. (A.9) and use Eq. (A.12) to yield

$$\begin{aligned} N_1(1+1/f_1^g)x_{1j}^g &= N_4(1+1/f_4^g)x_{4j}^g \\ &\quad + (\delta_{4j}-\delta_{2j})(\sigma_{b,j}^g+\sigma_{t,j}^g) + (-\delta_{1j}+\delta_{2j})(\sigma_{b,j}^g+\sigma_{t,j}^g) \\ &= N_4(1+1/f_4^g)x_{4j}^g + (\delta_{4j}-\delta_{1j})(\sigma_{b,j}^g+\sigma_{t,j}^g) \end{aligned} \tag{A.14}$$

and

$$N_1 x_{1j}^g = \frac{N_4(1+1/f_4^g)x_{4j}^g}{(1+1/f_1^g)} + \frac{(\delta_{4j}-\delta_{1j})(\sigma_{b,j}^g+\sigma_{t,j}^g)}{(1+1/f_1^g)}. \tag{A.15}$$

Using Eqs. (A.15), (A.13), and (A.11), the sum $\sum_{i=1}^{4} N_i x_{ij}^g$ is

$$\begin{aligned} \sum_{i=1}^{4} N_i x_{ij}^g &= \frac{N_4(1+1/f_4^g)x_{4j}^g}{(1+1/f_1^g)} + \frac{(\delta_{4j}-\delta_{1j})(\sigma_{b,j}^g+\sigma_{t,j}^g)}{(1+1/f_1^g)} \\ &\quad + \frac{N_4(1+1/f_4^g)x_{4j}^g}{(1+1/f_2^g)} + \frac{(\delta_{4j}-\delta_{2j})(\sigma_{b,j}^g+\sigma_{t,j}^g)}{(1+1/f_2^g)} \\ &\quad + \frac{N_4(1+1/f_4^g)x_{4j}^g}{(1+1/f_3^g)} + \frac{(\delta_{4j}-\delta_{3j})(\sigma_{b,j}^g+\sigma_{t,j}^g)}{(1+1/f_3^g)} + N_4 x_{4j}^g. \end{aligned} \tag{A.16}$$

Multiplying the last term by $(1+1/f_4^g)/(1+1/f_4^g)$, factoring, and rearranging yields

$$\sum_{i=1}^{4} N_i x_{ij}^g = N_4 \,(1+1/f_4^g) x_{4j}^g \left(\sum_{i=1}^{4} \frac{1}{(1+1/f_i^g)} \right) + (\sigma_{b,j}^g + \sigma_{t,j}^g) \left[\frac{(\delta_{4j} - \delta_{1j})}{(1+1/f_1^g)} + \frac{(\delta_{4j} - \delta_{2j})}{(1+1/f_2^g)} + \frac{(\delta_{4j} - \delta_{3j})}{(1+1/f_3^g)} \right]. \tag{A.17}$$

Applying Eq. (A.2) yields

$$\sum_{i=1}^{4} N_i x_{ij}^g = N_4 \,(1+1/f_4^g) x_{4j}^g \left(\sum_{i=1}^{4} \frac{1}{(1+1/f_i^g)} \right) + \left(\frac{\Sigma_{t,m}^g}{N_j} + \frac{\Sigma_{e,m}^g}{N_j} \right) \left[\frac{(\delta_{4j} - \delta_{1j})}{(1+1/f_1^g)} + \frac{(\delta_{4j} - \delta_{2j})}{(1+1/f_2^g)} + \frac{(\delta_{4j} - \delta_{3j})}{(1+1/f_3^g)} \right]. \tag{A.18}$$

Multiplying by N_j and summing again over nuclides yields

$$\begin{aligned}
\sum_{j=1}^{4} N_j \sum_{i=1}^{4} N_i x_{ij}^g &= N_1 \sum_{i=1}^{4} N_i x_{i1}^g + N_2 \sum_{i=1}^{4} N_i x_{i2}^g + N_3 \sum_{i=1}^{4} N_i x_{i3}^g + N_4 \sum_{i=1}^{4} N_i x_{i4}^g \\
&= N_1 N_4 \,(1+1/f_4^g) x_{41}^g \left(\sum_{i=1}^{4} \frac{1}{(1+1/f_i^g)} \right) \\
&+ (\Sigma_{t,m}^g + \Sigma_{e,m}^g) \left[\frac{(\delta_{41} - \delta_{11})}{(1+1/f_1^g)} + \frac{(\delta_{41} - \delta_{21})}{(1+1/f_2^g)} + \frac{(\delta_{41} - \delta_{31})}{(1+1/f_3^g)} \right] \\
&+ N_2 N_4 \,(1+1/f_4^g) x_{42}^g \left(\sum_{i=1}^{4} \frac{1}{(1+1/f_i^g)} \right) \\
&+ (\Sigma_{t,m}^g + \Sigma_{e,m}^g) \left[\frac{(\delta_{42} - \delta_{12})}{(1+1/f_1^g)} + \frac{(\delta_{42} - \delta_{22})}{(1+1/f_2^g)} + \frac{(\delta_{42} - \delta_{32})}{(1+1/f_3^g)} \right] \\
&+ N_3 N_4 \,(1+1/f_4^g) x_{43}^g \left(\sum_{i=1}^{4} \frac{1}{(1+1/f_i^g)} \right) \\
&+ (\Sigma_{t,m}^g + \Sigma_{e,m}^g) \left[\frac{(\delta_{43} - \delta_{13})}{(1+1/f_1^g)} + \frac{(\delta_{43} - \delta_{23})}{(1+1/f_2^g)} + \frac{(\delta_{43} - \delta_{33})}{(1+1/f_3^g)} \right] \\
&+ N_4^2 \,(1+1/f_4^g) x_{44}^g \left(\sum_{i=1}^{4} \frac{1}{(1+1/f_i^g)} \right) \\
&+ (\Sigma_{t,m}^g + \Sigma_{e,m}^g) \left[\frac{(\delta_{44} - \delta_{14})}{(1+1/f_1^g)} + \frac{(\delta_{44} - \delta_{24})}{(1+1/f_2^g)} + \frac{(\delta_{44} - \delta_{34})}{(1+1/f_3^g)} \right]
\end{aligned}$$

$$
\begin{aligned}
&= N_1 N_4 (1+1/f_4^g) x_{41}^g \left(\sum_{i=1}^{4} \frac{1}{(1+1/f_i^g)} \right) - \frac{\Sigma_{t,m}^g + \Sigma_{e,m}^g}{(1+1/f_1^g)} \\
&+ N_2 N_4 (1+1/f_4^g) x_{42}^g \left(\sum_{i=1}^{4} \frac{1}{(1+1/f_i^g)} \right) - \frac{\Sigma_{t,m}^g + \Sigma_{e,m}^g}{(1+1/f_2^g)} \\
&+ N_3 N_4 (1+1/f_4^g) x_{43}^g \left(\sum_{i=1}^{4} \frac{1}{(1+1/f_i^g)} \right) - \frac{\Sigma_{t,m}^g + \Sigma_{e,m}^g}{(1+1/f_3^g)} \\
&+ N_4^2 (1+1/f_4^g) x_{44}^g \left(\sum_{i=1}^{4} \frac{1}{(1+1/f_i^g)} \right) \\
&+ (\Sigma_{t,m}^g + \Sigma_{e,m}^g) \left[\frac{1}{(1+1/f_1^g)} + \frac{1}{(1+1/f_2^g)} + \frac{1}{(1+1/f_3^g)} \right] \\
&= N_4 (1+1/f_4^g) \left(N_1 x_{41}^g + N_2 x_{42}^g + N_3 x_{43}^g + N_4 x_{44}^g \right) \left(\sum_{i=1}^{4} \frac{1}{(1+1/f_i^g)} \right). \qquad \text{(A.19)}
\end{aligned}
$$

Rearranging Eq. (A.14) and specifying $j = 1$,

$$
N_1 x_{41}^g = \frac{N_1^2 (1+1/f_1^g) x_{11}^g}{N_4 (1+1/f_4^g)} + \frac{N_1 \sigma_{b,1}^g + N_1 \sigma_{t,1}^g}{N_4 (1+1/f_4^g)}; \qquad \text{(A.20)}
$$

rearranging Eq. (A.12) and specifying $j = 2$,

$$
N_2 x_{42}^g = \frac{N_2^2 (1+1/f_2^g) x_{22}^g}{N_4 (1+1/f_4^g)} + \frac{N_2 \sigma_{b,2}^g + N_2 \sigma_{t,2}^g}{N_4 (1+1/f_4^g)}; \qquad \text{(A.21)}
$$

and rearranging Eq. (A.10) and specifying $j = 3$,

$$
N_3 x_{43}^g = \frac{N_3^2 (1+1/f_3^g) x_{33}^g}{N_4 (1+1/f_4^g)} + \frac{N_3 \sigma_{b,3}^g + N_3 \sigma_{t,3}^g}{N_4 (1+1/f_4^g)}. \qquad \text{(A.22)}
$$

Using Eqs. (A.20), (A.21), and (A.22) in Eq. (A.19) yields

$$
\begin{aligned}
\sum_{j=1}^{4} N_j \sum_{i=1}^{4} N_i x_{ij}^g &= N_4 (1+1/f_4^g) \left(\frac{N_1^2 (1+1/f_1^g) x_{11}^g}{N_4 (1+1/f_4^g)} + \frac{N_1 \sigma_{b,1}^g + N_1 \sigma_{t,1}^g}{N_4 (1+1/f_4^g)} \right. \\
&+ \frac{N_2^2 (1+1/f_2^g) x_{22}^g}{N_4 (1+1/f_4^g)} + \frac{N_2 \sigma_{b,2}^g + N_2 \sigma_{t,2}^g}{N_4 (1+1/f_4^g)} \\
&\left. + \frac{N_3^2 (1+1/f_3^g) x_{33}^g}{N_4 (1+1/f_4^g)} + \frac{N_3 \sigma_{b,3}^g + N_3 \sigma_{t,3}^g}{N_4 (1+1/f_4^g)} + N_4 x_{44}^g \right) \left(\sum_{i=1}^{4} \frac{1}{(1+1/f_i^g)} \right) \\
&= \left(N_1^2 (1+1/f_1^g) x_{11}^g + N_2^2 (1+1/f_2^g) x_{22}^g \right. \\
&+ N_3^2 (1+1/f_3^g) x_{33}^g + N_4^2 (1+1/f_4^g) x_{44}^g \\
&\left. + N_1 \sigma_{b,1}^g + N_1 \sigma_{t,1}^g + N_2 \sigma_{b,2}^g + N_2 \sigma_{t,2}^g + N_3 \sigma_{b,3}^g + N_3 \sigma_{t,3}^g \right) \left(\sum_{i=1}^{4} \frac{1}{(1+1/f_i^g)} \right). \qquad \text{(A.23)}
\end{aligned}
$$

Using Eq. (A.2) yields

$$
\sum_{j=1}^{4} N_j \sum_{i=1}^{4} N_i x_{ij}^g = \left(\sum_{k=1}^{4} N_k^2 (1+1/f_k^g) x_{kk}^g + 3\Sigma_{t,m}^g + 3\Sigma_{e,m}^g \right) \left(\sum_{i=1}^{4} \frac{1}{(1+1/f_i^g)} \right). \qquad \text{(A.24)}
$$

As mentioned in Sec. III, Eq. (16) represents $I \times G$ matrix equations. The $4 \times G$ equations for $x_{kk}^g, k=1,\ldots 4, g=1,\ldots G$ can be written

$$\begin{cases} N_1(1+1/f_1^g)x_{11}^g - \sum_{i=1}^{4} N_i x_{i1}^g = -\sigma_{b,1}^g \\ N_2(1+1/f_2^g)x_{22}^g - \sum_{i=1}^{4} N_i x_{i2}^g = -\sigma_{b,2}^g \\ N_3(1+1/f_3^g)x_{33}^g - \sum_{i=1}^{4} N_i x_{i3}^g = -\sigma_{b,3}^g \\ N_4(1+1/f_4^g)x_{44}^g - \sum_{i=1}^{4} N_i x_{i4}^g = -\sigma_{b,4}^g. \end{cases} \tag{A.25}$$

Multiplying each line k of Eq. (A.25) by N_k and rearranging yields

$$\begin{cases} N_1^2(1+1/f_1^g)x_{11}^g = -N_1\sigma_{b,1}^g + N_1\sum_{i=1}^{4} N_i x_{i1}^g \\ N_2^2(1+1/f_2^g)x_{22}^g = -N_2\sigma_{b,2}^g + N_2\sum_{i=1}^{4} N_i x_{i2}^g \\ N_3^2(1+1/f_3^g)x_{33}^g = -N_3\sigma_{b,3}^g + N_3\sum_{i=1}^{4} N_i x_{i3}^g \\ N_4^2(1+1/f_4^g)x_{44}^g = -N_4\sigma_{b,4}^g + N_4\sum_{i=1}^{4} N_i x_{i4}^g. \end{cases} \tag{A.26}$$

Adding each line of Eq. (A.26) and using Eq. (A.1) yields

$$\begin{aligned} \sum_{k=1}^{4} N_k^2(1+1/f_k^g)x_{kk}^g &= -\sum_{k=1}^{4} N_k\sigma_{b,k}^g + \sum_{k=1}^{4} N_k \sum_{i=1}^{4} N_i x_{ik}^g \\ &= -3\Sigma_{t,m}^g - 4\Sigma_{e,m}^g + \sum_{k=1}^{4} N_k \sum_{i=1}^{4} N_i x_{ik}^g, \end{aligned} \tag{A.27}$$

or

$$\sum_{k=1}^{4} N_k^2(1+1/f_k^g)x_{kk}^g + 3\Sigma_{t,m}^g + 3\Sigma_{e,m}^g = -\Sigma_{e,m}^g + \sum_{k=1}^{4} N_k \sum_{i=1}^{4} N_i x_{ik}^g. \tag{A.28}$$

Using Eq. (A.28) on the right side of Eq. (A.24) and reintroducing $x_{ij}^g \equiv \partial\sigma_{t,i}^g / \partial N_j$ yields

$$\sum_{j=1}^{4} N_j \sum_{i=1}^{4} N_i \frac{\partial\sigma_{t,i}^g}{\partial N_j} = \left(-\Sigma_{e,m}^g + \sum_{k=1}^{4} N_k \sum_{i=1}^{4} N_i \frac{\partial\sigma_{t,i}^g}{\partial N_k}\right)\left(\sum_{i=1}^{4} \frac{1}{(1+1/f_i^g)}\right). \tag{A.29}$$

Rearranging Eq. (A.29) yields

$$\sum_{j=1}^{4} N_j \sum_{i=1}^{4} N_i \frac{\partial\sigma_{t,i}^g}{\partial N_j} = -\Sigma_{e,m}^g \frac{\sum_{i=1}^{4} \frac{f_i^g}{(f_i^g+1)}}{1-\sum_{i=1}^{4} \frac{f_i^g}{(f_i^g+1)}}. \tag{A.30}$$

Equation (A.30) was derived for $I = 4$. For $I = 1$, $\sigma_{b,1}^g = 0$ from Eqs. (4) and (5) and $\partial\sigma_{t,1}^g / \partial N_1 = 0$ from Eq. (8). For $I > 1$, the derivation is the same as in this appendix. Therefore

$$\sum_{j=1}^{I} N_j \sum_{i=1}^{I} N_i \frac{\partial \sigma_{t,i}^g}{\partial N_j} = -\Sigma_{e,m}^g \frac{\sum_{i=1}^{I} \frac{f_i^g}{(f_i^g+1)}}{1-\sum_{i=1}^{I} \frac{f_i^g}{(f_i^g+1)}},\ g=1,\ldots G. \quad \text{(A.31)}$$

If the escape cross section $\Sigma_{e,m}^g$ is zero, then Eq. (21) in the main text is satisfied.

The same can be shown for $\partial \sigma_{b,i}^g / \partial N_j$. Take the derivative of the left side of Eq. (A.1) with respect to N_j:

$$\begin{aligned} \frac{\partial}{\partial N_j} \sum_{i=1}^{I} N_i \sigma_{b,i}^g &= \sum_{i=1}^{I} \frac{\partial N_i}{\partial N_j} \sigma_{b,i}^g + \sum_{i=1}^{I} N_i \frac{\partial \sigma_{b,i}^g}{\partial N_j} \\ &= \sum_{i=1}^{I} \delta_{ij} \sigma_{b,i}^g + \sum_{i=1}^{I} N_i \frac{\partial \sigma_{b,i}^g}{\partial N_j} \\ &= \sigma_{b,j}^g + \sum_{i=1}^{I} N_i \frac{\partial \sigma_{b,i}^g}{\partial N_j}. \end{aligned} \quad \text{(A.32)}$$

The same steps can be done with the right side of Eq. (A.1) [using Eq. (4)] to yield

$$(I-1)\frac{\partial}{\partial N_j} \sum_{i=1}^{I} N_i \sigma_{t,i}^g = (I-1)\sigma_{t,j}^g + (I-1)\sum_{i=1}^{I} N_i \frac{\partial \sigma_{t,i}^g}{\partial N_j}. \quad \text{(A.33)}$$

Note that $\partial \Sigma_{e,m}^g / \partial N_j = 0$. Multiply Eq. (A.32) by N_j and sum over nuclides:

$$\sum_{j=1}^{I} N_j \frac{\partial}{\partial N_j} \sum_{i=1}^{I} N_i \sigma_{b,i}^g = \sum_{j=1}^{I} N_j \sigma_{b,j}^g + \sum_{j=1}^{I} N_j \sum_{i=1}^{I} N_i \frac{\partial \sigma_{b,i}^g}{\partial N_j}. \quad \text{(A.34)}$$

Again, the same steps can be done with Eq. (A.33) to yield

$$(I-1)\sum_{j=1}^{I} N_j \frac{\partial}{\partial N_j} \sum_{i=1}^{I} N_i \sigma_{t,i}^g = (I-1)\sum_{j=1}^{I} N_j \sigma_{t,j}^g + (I-1)\sum_{j=1}^{I} N_j \sum_{i=1}^{I} N_i \frac{\partial \sigma_{t,i}^g}{\partial N_j}. \quad \text{(A.35)}$$

From Eq. (A.1), the left sides of Eqs. (A.34) and (A.35) are equal. Equating the right sides and using Eq. (A.1) again yields

$$\sum_{j=1}^{I} N_j \sum_{i=1}^{I} N_i \frac{\partial \sigma_{b,i}^g}{\partial N_j} = (I-1)\sum_{j=1}^{I} N_j \sum_{i=1}^{I} N_i \frac{\partial \sigma_{t,i}^g}{\partial N_j}. \quad \text{(A.36)}$$

Using Eq. (A.31) yields

$$\sum_{j=1}^{I} N_j \sum_{i=1}^{I} N_i \frac{\partial \sigma_{b,i}^g}{\partial N_j} = -(I-1)\Sigma_{e,m}^g \frac{\sum_{i=1}^{I} \frac{f_i^g}{(f_i^g+1)}}{1-\sum_{i=1}^{I} \frac{f_i^g}{(f_i^g+1)}},\ g=1,\ldots G. \quad \text{(A.37)}$$

If the escape cross section $\Sigma_{e,m}^g$ is zero, then Eq. (22) in the main text is satisfied.

The same can be shown for any reaction rate $\partial \sigma_{x,i}^g / \partial N_j$. Define

$$f_{x,i}^g \equiv \frac{1}{2\sqrt{\sigma_{b,i}^g}} \frac{\hat{\sigma}_{x,i}^g(\hat{s}_{0,h}) - \hat{\sigma}_{x,i}^g(\hat{s}_{0,h-1})}{\sqrt{\hat{s}_{0,h}} - \sqrt{\hat{s}_{0,h-1}}} \quad \text{(A.38)}$$

so that Eq. (19) becomes

$$\frac{\partial \sigma_{x,i}^g}{\partial N_j} = f_{x,i}^g \frac{\partial \sigma_{b,i}^g}{\partial N_j}. \tag{A.39}$$

Using Eq. (10) yields

$$\frac{\partial \sigma_{x,i}^g}{\partial N_j} = f_{x,i}^g \left(-\frac{\delta_{ij}}{N_i^2}(\Sigma_{t,m}^g + \Sigma_{e,m}^g) + \frac{1}{N_i}\sigma_{t,j}^g(\sigma_{b,j}^g) + \frac{1}{N_i}\sum_{k=1}^{I} N_k \frac{\partial \sigma_{t,k}^g}{\partial N_j} - \frac{\partial \sigma_{t,i}^g}{\partial N_j} \right). \tag{A.40}$$

Multiplying both sides by N_i and summing over *i* yields

$$\begin{aligned}\sum_{i=1}^{I} N_i \frac{\partial \sigma_{x,i}^g}{\partial N_j} &= -\sum_{i=1}^{I} f_{x,i}^g \frac{\delta_{ij}}{N_i}(\Sigma_{t,m}^g + \Sigma_{e,m}^g) + \left(\sum_{i=1}^{I} f_{x,i}^g\right)\sigma_{t,j}^g(\sigma_{b,j}^g) + \left(\sum_{i=1}^{I} f_{x,i}^g\right)\sum_{k=1}^{I} N_k \frac{\partial \sigma_{t,k}^g}{\partial N_j} - \sum_{i=1}^{I} f_{x,i}^g N_i \frac{\partial \sigma_{t,i}^g}{\partial N_j} \\ &= -f_{x,j}^g \frac{1}{N_j}(\Sigma_{t,m}^g + \Sigma_{e,m}^g) + \left(\sum_{i=1}^{I} f_{x,i}^g\right)\sigma_{t,j}^g(\sigma_{b,j}^g) + \left(\sum_{i=1}^{I} f_{x,i}^g\right)\sum_{k=1}^{I} N_k \frac{\partial \sigma_{t,k}^g}{\partial N_j} - \sum_{i=1}^{I} f_{x,i}^g N_i \frac{\partial \sigma_{t,i}^g}{\partial N_j}.\end{aligned} \tag{A.41}$$

Multiplying both sides by N_j and summing over *j* yields

$$\begin{aligned}\sum_{j=1}^{I} N_j \sum_{i=1}^{I} N_i \frac{\partial \sigma_{x,i}^g}{\partial N_j} &= -\left(\sum_{j=1}^{I} f_{x,j}^g\right)\Sigma_{t,m}^g - \left(\sum_{j=1}^{I} f_{x,j}^g\right)\Sigma_{e,m}^g + \left(\sum_{i=1}^{I} f_{x,i}^g\right)\sum_{j=1}^{I} N_j \sigma_{t,j}^g(\sigma_{b,j}^g) \\ &\quad + \left(\sum_{i=1}^{I} f_{x,i}^g\right)\sum_{j=1}^{I} N_j \sum_{k=1}^{I} N_k \frac{\partial \sigma_{t,k}^g}{\partial N_j} - \sum_{j=1}^{I} N_j \sum_{i=1}^{I} f_{x,i}^g N_i \frac{\partial \sigma_{t,i}^g}{\partial N_j}.\end{aligned} \tag{A.42}$$

The first and third terms on the right side cancel because of Eq. (4). Introducing Eq. (A.31) yields

$$\begin{aligned}\sum_{j=1}^{I} N_j \sum_{i=1}^{I} N_i \frac{\partial \sigma_{x,i}^g}{\partial N_j} &= -\left(\sum_{j=1}^{I} f_{x,j}^g\right)\Sigma_{e,m}^g - \left(\sum_{i=1}^{I} f_{x,i}^g\right)\Sigma_{e,m}^g \frac{\displaystyle\sum_{i=1}^{I} \frac{f_i^g}{(f_i^g+1)}}{1 - \displaystyle\sum_{i=1}^{I} \frac{f_i^g}{(f_i^g+1)}} - \sum_{j=1}^{I} N_j \sum_{i=1}^{I} f_{x,i}^g N_i \frac{\partial \sigma_{t,i}^g}{\partial N_j} \\ &= -\left(\sum_{j=1}^{I} f_{x,j}^g\right)\Sigma_{e,m}^g \left(1 + \frac{\displaystyle\sum_{i=1}^{I} \frac{f_i^g}{(f_i^g+1)}}{1 - \displaystyle\sum_{i=1}^{I} \frac{f_i^g}{(f_i^g+1)}} \right) - \sum_{j=1}^{I} N_j \sum_{i=1}^{I} f_{x,i}^g N_i \frac{\partial \sigma_{t,i}^g}{\partial N_j} \\ &= -\Sigma_{e,m}^g \left(\frac{\displaystyle\sum_{j=1}^{I} f_{x,j}^g}{1 - \displaystyle\sum_{i=1}^{I} \frac{f_i^g}{(f_i^g+1)}} \right) - \sum_{j=1}^{I} N_j \sum_{i=1}^{I} f_{x,i}^g N_i \frac{\partial \sigma_{t,i}^g}{\partial N_j}.\end{aligned} \tag{A.43}$$

Applying Eqs. (8) and (9) yields

$$\sum_{j=1}^{I} N_j \sum_{i=1}^{I} N_i \frac{\partial \sigma_{x,i}^g}{\partial N_j} = -\Sigma_{e,m}^g \left(\frac{\displaystyle\sum_{j=1}^{I} f_{x,j}^g}{1 - \displaystyle\sum_{i=1}^{I} \frac{f_i^g}{(f_i^g+1)}} \right) - \sum_{j=1}^{I} N_j \sum_{i=1}^{I} N_i f_{x,i}^g f_i^g \frac{\partial \sigma_{b,i}^g}{\partial N_j}. \tag{A.44}$$

But from Eq. (A.39), we must also have

$$\sum_{j=1}^{I} N_j \sum_{i=1}^{I} N_i \frac{\partial \sigma_{x,i}^g}{\partial N_j} = \sum_{j=1}^{I} N_j \sum_{i=1}^{I} N_i f_{x,i}^g \frac{\partial \sigma_{b,i}^g}{\partial N_j}. \tag{A.45}$$

If the escape cross section $\Sigma_{e,m}^{g}$ is zero, then the only way to satisfy Eqs. (A.44) and (A.45) is if Eq. (23) in the main text is satisfied.

References

19. Eric W. Weisstein, "Augmented Matrix," from MathWorld—A Wolfram Web Resource, https://mathworld.wolfram.com/AugmentedMatrix.html, accessed Aug. 16, 2020.

Appendix B
Input Files for the Test Problems

SENSMG Input File for the UO_2 Sphere with Water (Sec. VII.A)

```
Saller's prob. 2
sphere keff
test
2 / no of materials
1 92235 0.004903468 92238 0.019613872 8016 0.049034681 / UO2
2 1001 0.066656016 8016 0.033328008 / water
 0.073552021 0.099984024 / densities
2 / no of shells
 35.  45.
  1    2    / material nos
 0          / number of edit points
 0          / number of reaction-rate ratios
 0          / number of njoy reactions
```

SENSMG Input File for the Green Block Critical Experiment (Sec. VII.B)

```
raffety and mihalczo u(2)f4-2 unreflected green block, sphere by williams
sphere keff
e8g44s
1 / no of materials
1 6012 1.857768E-02 6013 2.009312E-04 9019 2.628098E-02 92235 1.330519E-04 92238 6.437193E-03 1001
3.905952E-02 /
 9.06893561E-02 / densities
1 / no of shells
 38.5
  1         / material nos
 0          / number of edit points
 0          / number of reaction-rate ratios
 0          / number of njoy reactions
```

MCNP Input File for the Green Block Critical Experiment (Sec. VII.B)

```
raffety and mihalczo u(2)f4-2 unreflected green block, sphere by williams
1  1  9.06893561E-02   -1    imp:n,p=1
99 0                    1    imp:n,p=0

1  so  38.5

mode n
totnu
c kcode 1e7 1. 50 1050
kcode 1e6 1. 50 1050
prdmp j 500
rand gen=2 seed=1000041
sdef pos=0. 0. 0. rad=d1 erg=d2
si1 0. 38.5
sp1 -21 2
sp2 -3 0.988 2.249
m1    1001.00c  3.905952E-02
      6012.00c  1.857768E-02
      6013.00c  2.009312E-04
      9019.00c  2.628098E-02
      92235.00c 1.330519E-04
      92238.00c 6.437193E-03
mt1   h-poly.40t
print -30
kopts  blocksize=5  kinetics=yes  precursor=yes
ksen001  xs  cell=  1
ksen002  xs  cell=  1
         erg=1.000000E-11 3.000000E-09 7.500000E-09 1.000000E-08 2.530000E-08
             3.000000E-08 4.000000E-08 5.000000E-08 7.000000E-08 1.000000E-07
             1.500000E-07 2.000000E-07 2.250000E-07 2.500000E-07 2.750000E-07
             3.250000E-07 3.500000E-07 3.750000E-07 4.000000E-07 6.250000E-07
             1.000000E-06 1.770000E-06 3.000000E-06 4.750000E-06 6.000000E-06
             8.100000E-06 1.000000E-05 3.000000E-05 1.000000E-04 5.500000E-04
             3.000000E-03 1.700000E-02 2.500000E-02 1.000000E-01 4.000000E-01
             9.000000E-01 1.400000E+00 1.850000E+00 2.354000E+00 2.479000E+00
             3.000000E+00 4.800000E+00 6.434000E+00 8.187300E+00 2.000000E+01
```